2. Methods

2.1. Surgical preparation

Animal care was provided in strict accordance with the Guiding Principles for the Care and Use of Animals in the Field of Physiological Sciences approved by the Physiological Society of Japan. All protocols were reviewed and approved by the Animal Subject Committee at the National Cerebral and Cardiovascular Center. Male Wistar Kyoto rats weighing from 310 to 460 g were anesthetized by an intraperitoneal injection of pentobarbital sodium (50 mg/kg) and ventilated mechanically via a tracheal tube with oxygen-enriched room air. The depth of anesthesia was maintained by continuous intravenous infusion of pentobarbital sodium (20–25 mg kg^{-1} h^{-1}) through a double lumen catheter inserted into the right external carotid vein. Ringer solution (6 mg kg^{-1} h^{-1}) was administered to maintain fluid balance. Arterial blood pressure (AP) was measured using a catheter inserted into the right common carotid artery. Heart rate (HR) was determined from AP using a cardiotachometer. Body temperature was maintained at approximately 38 °C using a heating pad.

2.2. MA and EA stimulations ($n=9$)

With the animal in the supine position, both hind limbs were lifted to obtain a better view of the lateral sides of the lower legs. An acupuncture needle with a diameter of 0.2 mm (CE0123, Seirin-Kasei, Japan) was inserted into a point below the knee joint just lateral to the tibia in the left or right leg. For MA stimulation, the acupuncture needle was inserted to a depth of 5–10 mm and manually twisted clockwise and counter-clockwise, and moved up and down at a frequency of 1–2 Hz for a duration of 120 s. Two to three MA trials were conducted with an intervening interval of more than 5 min within which AP and HR returned to the respective pre-stimulation values. For EA stimulation, another acupuncture needle was inserted into a point approximately 1 cm from the above-mentioned needle toward the ankle joint and used as the ground. EA was applied for 120 s using an isolator connected to an electrical stimulator (SEN 7203, Nihon Kohden, Japan). The pulse width and the stimulus current were set at 500 μs and 5 mA, respectively. The stimulation frequency was set at 10 Hz in six and at 20 Hz in three of the nine rats. The pulse duration was based on previous studies (Tjen-A-Looi et al., 2005; Yamamoto et al., 2008; Uchida et al., 2008). The amplitude and frequency were selected so that the magnitudes of reflex hemodynamic responses became comparable to those induced by MA before gadolinium administration. In each animal, two to three EA trials were conducted with an intervening interval of more than 5 min within which AP and HR returned to the respective pre-stimulation values.

Gadolinium chloride hexahydrate was dissolved in saline at a concentration of 20 mM (Nakamoto and Matsukawa, 2007). After performing MA and EA under control conditions, we administered the gadolinium solution intravenously (2 ml/kg). After 10 min, we repeated MA and EA. The acupuncture needle positions were kept unchanged between MA and EA trials as well as before and after the gadolinium administration.

In a supplemental protocol ($n=7$ additional rats), to examine the possibility that simple insertion of needles caused significant hemodynamic influences, an acupuncture needle (CE0123, Seirin-Kasei, Japan) was only inserted into a point below the knee joint just lateral to the tibia in the left or right leg and placed for a duration of 120 s. Needle was inserted to a depth of 5–10 mm.

2.3. Aortic depressor nerve stimulation ($n=6$)

Using a pair of platinum electrodes, we identified the aortic depressor nerve (ADN) running along the common carotid artery, based on the AP pulse-synchronous nerve activity monitored through a loud speaker. After a depressor response to brief electrical stimulation of the nerve was confirmed, the electrodes and the nerve were fixed and insulated by silicone glue (Kwik-Sil, World Precision Instruments, FL, USA). The nerve fibers caudal to the electrodes were then crushed by a tight ligature so that only the afferent fibers directed to the central nervous system were stimulated. In four of the six rats, the right ADN was stimulated. In the remaining two rats, the left ADN was stimulated because of failure to stimulate the right ADN properly. The ADN was stimulated for 120 s at a frequency of 50 Hz (pulse width: 2 ms, voltage: 2 V). ADN stimulation was repeated with an interval of 5 min until the AP and HR responses appeared to be reproducible under control conditions. We then administered the gadolinium solution intravenously (20 mM, 2 ml/kg). After 10 min, we repeated the ADN stimulation.

2.4. Data analysis

Data were digitized using a 16-bit analog-to-digital converter (Contec, Japan) and stored at 200 Hz on a laboratory computer system. First, AP and HR data were averaged every 10 s. Averaged time courses of AP and HR responses were then obtained from two to three trials of MA, EA or ADN stimulation in each animal. Next, the effects of MA, EA or ADN were examined using repeated-measures one-way analysis of variance (ANOVA) followed by Dunnett's test (Glantz, 2002). The baseline data point immediately before stimulation was treated as a single control point for the Dunnett's test. Finally, the maximum effect of MA, EA or ADN stimulation was quantified by the differences between the minimum and baseline values for AP and HR (ΔAP and ΔHR). The effects of gadolinium on ΔAP and ΔHR were examined by a paired-t test (Glantz, 2002). The differences were considered significant at $P<0.05$. Data are presented in mean ± SE values.

3. Results

Fig. 1 depicts the averaged time courses of AP and HR responses to MA ($n=9$ rats). MA gradually decreased AP and HR under control conditions. The minimum AP and HR were reached near the end of the MA stimulation period. After the cessation of MA, AP and HR gradually returned toward the respective baseline values. Intravenous gadolinium administration significantly decreased baseline AP from 138 ± 5 to 120 ± 5 mm Hg ($P<0.01$) but had no significant effect on baseline HR (379 ± 10 vs. 383 ± 7 bpm). Following gadolinium administration, although MA also decreased AP and HR significantly, ΔAP tended to be attenuated (−30 ± 5 vs. −18 ± 4 mm Hg; 68 ± 16% of the pre-gadolinium; $P=0.06$) and ΔHR was significantly attenuated (−22 ± 5 vs. −10 ± 3 bpm; 57 ± 23% of the pre-gadolinium; $P<0.05$) compared to control conditions.

Fig. 2 depicts the averaged time courses of AP and HR responses to EA ($n=9$ rats). Under control conditions, EA decreased AP and HR. Both responses reached almost a steady state at approximately 1 min of EA stimulation. AP and HR remained decreased during the rest of the EA stimulation period, and gradually returned toward the respective baseline values after the cessation of EA. Intravenous gadolinium administration significantly decreased baseline AP from 140 ± 5 to 123 ± 7 mm Hg ($P<0.01$) but did not affect baseline HR (385 ± 9 vs. 384 ± 7 bpm). Following gadolinium administration, although EA significantly decreased AP, the decrease in HR was only significant at 55 s of EA stimulation. ΔAP (−32 ± 6 vs. −15 ± 5 mm Hg; 38 ± 11% of the pre-gadolinium; $P<0.01$) and ΔHR (−22 ± 5 vs. −9 ± 4 bpm; 37 ± 14% of the pre-gadolinium; $P<0.01$) were attenuated significantly compared to control conditions.

In the supplemental protocol ($n=7$ rats), the insertion of an acupuncture needle alone did not significantly change AP (138 ± 9 vs.138 ± 9 mm Hg) or HR (399 ± 20 vs. 400 ± 20 bpm).

Fig. 3 shows the averaged time courses of AP and HR responses to ADN stimulation ($n=6$ rats). ADN stimulation decreased AP and HR under control conditions. The minimum AP and HR were reached at 15 s of ADN stimulation. Both parameters remained decreased during the rest of the ADN stimulation period, and returned toward the respective

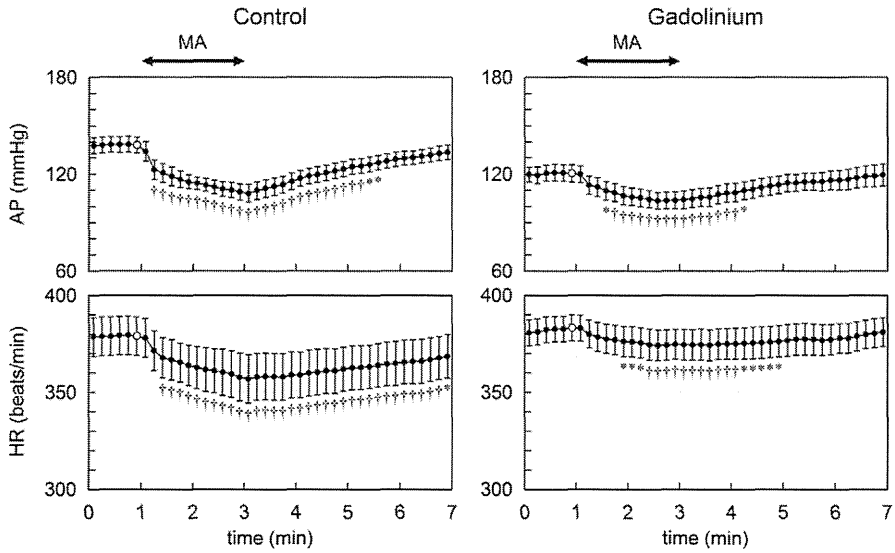

Fig. 1. Time courses of arterial pressure (AP) and heart rate (HR) responses induced by manual acupuncture (MA) averaged from 9 rats. MA gradually decreased AP and HR under control conditions (left) and after gadolinium administration (right). Gadolinium treatment tended to attenuate the AP response and significantly attenuated the HR response induced by MA, compared to control conditions. Data are mean ± SE values. *P<0.05 and †P<0.01 versus the control data point (open circle) immediately before the application of MA.

baseline values after the cessation of ADN stimulation. AP and HR appeared to recover more rapidly compared to those observed after MA and EA. Intravenous gadolinium administration significantly decreased baseline AP from 126 ± 4 to 118 ± 2 mm Hg (P<0.01) but had no significant effect on baseline HR (373 ± 13 vs. 369 ± 11 bpm). Following gadolinium administration, ADN stimulation significantly decreased AP and HR. Neither ΔAP (−43 ± 7 vs. −49 ± 3 mm Hg) nor ΔHR (−27 ± 8 vs. −34 ± 5 bpm) was attenuated compared to control conditions.

4. Discussion

We have shown that ion channels blocked by gadolinium are implicated in the hypotensive and bradycardic effects of acupuncture at the hind limb in rats, irrespective of technique.

4.1. Effects of gadolinium on AP and HR responses to MA and EA

Insertion of acupuncture needle alone did not change AP and HR significantly, indicating that continuous stimulation either by MA or EA was necessary to induce sustained AP and HR responses. Mechanoreceptors are thought to play an important role in the sensory mechanism of MA. Because gadolinium blocks mechanosensitive ion channels in sensory neurons (Cho et al., 2002), we hypothesized that intravenous administration of gadolinium would attenuate the AP and HR responses to MA. As expected, ΔAP tended to be attenuated after gadolinium administration (Fig. 1, top). However, since gadolinium also decreased baseline AP, it is uncertain whether the attenuation of ΔAP was mainly attributable to the inhibition of reflex response to MA or to the decreased baseline AP. On the other hand, gadolinium did not significantly affect baseline HR and

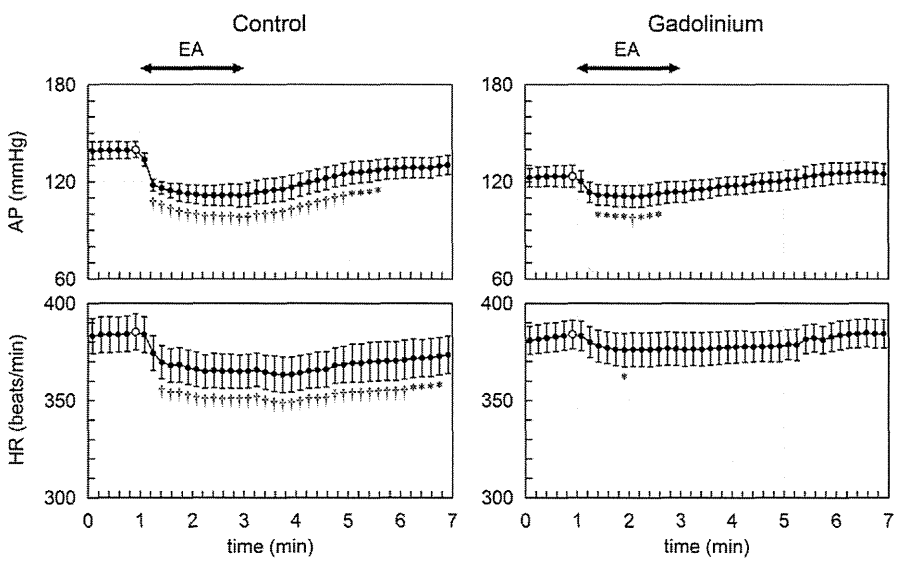

Fig. 2. Time courses of AP and HR responses induced by electroacupuncture (EA) averaged from 9 rats. EA gradually decreased AP and HR under control conditions (left) and after gadolinium administration (right). Gadolinium significantly attenuated both AP and HR responses induced by EA, compared to control conditions. Data are mean ± SE values. *P<0.05 and †P<0.01 versus the control data point (open circle) immediately before the application of EA.

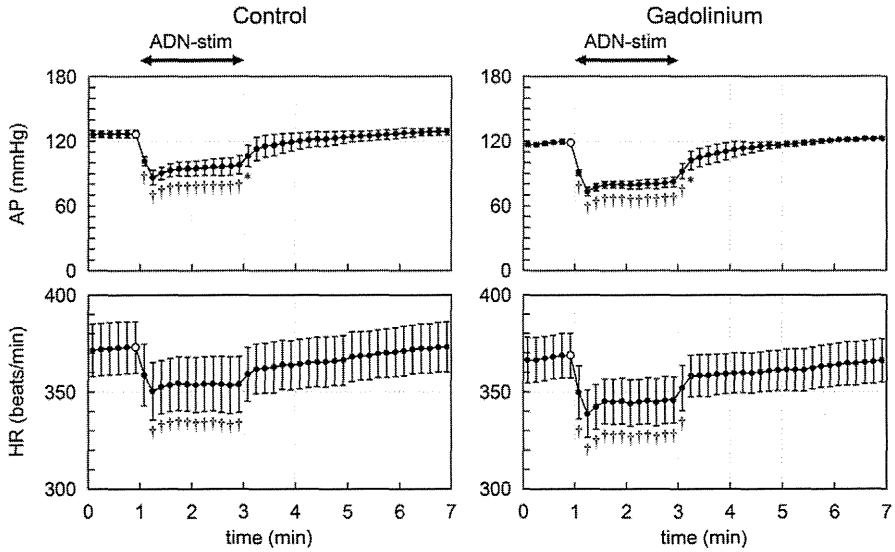

Fig. 3. Time courses of AP and HR responses induced by electrical stimulation of the aortic depressor nerve (ADN-stim) averaged from 6 rats. ADN-stim decreased AP and HR under control conditions (left) and after gadolinium administration (right). Gadolinium did not attenuate the AP and HR responses induced by ADN-stim, compared to control conditions. Data are mean ± SE values. $^{*}P<0.05$ and $^{\dagger}P<0.01$ versus the control data point (open circle) immediately before the application of ADN-stim.

significantly attenuated ΔHR induced by MA (Fig. 1, bottom). Judging from the HR response, it is conceivable that gadolinium inhibits the reflex hemodynamic responses to MA.

We assumed that direct depolarization of sensory axons and nerve terminals adjacent to the needle could be the major sensory mechanism of EA. In fact, direct electrical stimulation of muscle afferent fibers evokes a variety of cardiovascular responses similar to those induced by EA (Sato et al., 1981). If direct depolarization is the major sensory mechanism for EA, inhibition of mechanoreceptors would have no significant effect on EA, because the results of the ADN stimulation protocol indicates that the axonal conduction would not be blocked even after gadolinium administration once the afferent nerve is discharged (Fig. 3). Contrary to this assumption, gadolinium significantly attenuated ΔAP and ΔHR induced by EA (Fig. 2), suggesting that the mechanoreceptors play an important role in the sensory mechanism of EA, as in the case of MA. EA probably causes electrical twitching of surrounding tissues and exerts MA-like stimulation through the mechanoreceptors.

Despite the significant contribution of mechanoreceptors to the sensory mechanisms of both MA and EA, the fact that the hemodynamic responses to MA and EA were not entirely abrogated after gadolinium administration indicates the presence of sensory mechanisms other than the mechanosensitive ion channels. Not all capsaicin-sensitive neurons are mechanosensitive, and gadolinium has no effect on capsaicin-induced calcium transient in sensory neurons (Gschossmann et al., 2000). Depletion of group IV fibers by neonatal capsaicin treatment reduces the influence of EA on the pressor responses to mechanical stimulation of visceral organs (Tjen-A-Looi et al., 2005), suggesting an importance of capsaicin-sensitive neurons in the mechanisms of acupuncture. Nociceptive neurons are therefore a likely candidate for the residual sensory mechanism after gadolinium administration. The group IV C-fiber tactile afferents is known to be widely distributed in the skin of mammals (Wessberg et al., 2003). These fibers could be regarded as a cutaneous intrinsic visceral afferent nervous system (Silberstein, 2009). In addition, the present results do not rule out the possibility that direct depolarization of sensory axons or nerve terminals occurs during EA. Albeit this assumption, EA seemed to have received even greater influence from gadolinium than MA (Figs. 1 and 2). Because MA with needle movements can cause greater deformations in the adjacent extracellular milieu compared to EA, MA may have induced signal transductions other than mechanosensitive ion channels, such as integrin-linked signal transduction pathways (Aplin et al., 1998), resulting in the greater residual hemodynamic responses after gadolinium administration. Further studies are required in the future to solve this question.

4.2. Effects of gadolinium on the AP and HR responses to ADN stimulation

Gadolinium decreased baseline AP, suggesting actions other than the inhibition of mechanosensitive ion channels. For instance, gadolinium has been shown to block voltage-gated calcium, sodium and potassium channels (Adding et al., 2001). To exclude the possibility that gadolinium attenuates the reflex hemodynamic responses to MA and EA via nonspecific mechanisms such as the inhibition of central autonomic neurotransmission, we performed the ADN stimulation experiment. Gadolinium did not attenuate ΔAP and ΔHR induced by ADN stimulation (Fig. 3). It is unlikely, therefore, that gadolinium inhibits the central autonomic neurotransmission from afferent to efferent nerve activities or significantly blunted the AP and HR responses to changes in autonomic nerve activities.

4.3. Implication of MA and EA

Although the present results indicate that MA and EA may share a common sensory mechanism, EA may be more flexible than MA in terms of its application for biomedical engineering because the effects of EA can be controlled quantitatively by adjusting the stimulation current and stimulation frequency. As an example, a previous study from our laboratories has demonstrated that servo-controlled hind limb electrical stimulation can reduce AP at a prescribed target level in anesthetized cats (Kawada et al., 2009). EA can be applied continuously using a stimulating device without the attendance of an acupuncturist once the needle is properly positioned. Continuous electrical stimulation of auricular acupuncture points for 48 h/week has been shown to be more effective than auricular acupuncture without electrical stimulation for the treatment of chronic cervical pain in an outpatient population (Sator-Katzenschlager et al., 2003). Although further studies are required, EA delivered via a dedicated stimulating device may be an additional modality to the treatment of cardiovascular diseases.

4.4. Limitations

First, the present study was conducted under pentobarbital anesthesia. Because anesthesia affects the autonomic tone, AP and HR

responses may differ when different anesthetics are used or when the animals are in a conscious state. However, as we compared the effects of gadolinium on the reflex responses to MA and EA under the same anesthetic conditions, the interpretation of the sensory mechanisms for MA and EA should be valid. Second, we performed EA at frequencies of 10 or 20 Hz in order to obtain AP and HR responses comparable to those observed during MA under control conditions. Because the effects of EA may differ depending on the magnitude of stimulation including pulse duration, current and frequency (Uchida et al., 2008; Kawada et al., 2009), further studies are needed to examine whether the effects of gadolinium on EA-induced hemodynamic responses vary depending on the stimulation intensities.

4.5. Conclusion

Intravenous administration of gadolinium attenuated the AP and HR responses to both MA and EA, suggesting that the mechanosensitive ion channels are involved in the sensory mechanisms of both MA and EA. EA may cause electrical twitching of surrounding tissues and induce MA-like stimulation through mechanoreceptors.

Acknowledgments

This study was supported by Health and Labour Sciences Research Grants (H19-nano-Ippan-009, H20-katsudo-Shitei-007, and H21-nano-Ippan-005) from the Ministry of Health, Labour and Welfare of Japan; by a Grant-in-Aid for Scientific Research (No. 20390462) from the Ministry of Education, Culture, Sports, Science and Technology of Japan; and by the Industrial Technology Research Grant Program from the New Energy and Industrial Technology Development Organization (NEDO) of Japan.

Appendix A

In an attempt to demonstrate that gadolinium does not significantly affect the hemodynamic responses to direct nerve stimulation related to acupuncture at the hind limb, we performed an additional protocol of tibial nerve stimulation in 5 anesthetized rats. The right tibial nerve was exposed and placed on a pair of platinum electrodes, and was stimulated for 120 s (500 μs, 10 Hz, 2 or 5 mA). ΔAP was -10.5 ± 3.5 mm Hg under baseline conditions, which was attenuated to -8.2 ± 4.4 mm Hg after gadolinium administration ($74 \pm 15\%$ of the pre-gadolinium, $P<0.01$). Although the relative reduction seemed smaller than that observed in EA ($38 \pm 11\%$ of the pre-gadolinium, see main text), because the reduction of ΔAP could be partly attributable to the decreased baseline AP after gadolinium administration, we could not judge whether gadolinium had truly inhibited the hypotensive effect of tibial nerve stimulation. Unfortunately, the tibial nerve stimulation did not change HR significantly in our experimental conditions ($\Delta HR = -1.1 \pm 4.4$ bpm before gadolinium vs. $\Delta HR = -1.4 \pm 4.1$ bpm after gadolinium), as opposed to a previous study (Uchida et al., 2008). As a result, we could not judge the effect of gadolinium based on HR either. We think the ADN stimulation protocol in the main text would be a second best surrogate to indicate the inability of gadolinium to block hemodynamic responses induced by direct activation of the afferent nerve.

References

Adding, L.C., Bannenberg, G.L., Gustafsson, L.E., 2001. Basic experimental studies and clinical aspects of gadolinium salts and chelates. Cardiovasc. Drug Rev. 19, 41–56.
Aplin, A.E., Howe, A., Alahari, S.K., Juliano, R.L., 1998. Signal transduction and signal modulation by cell adhesion receptors: the role of integrins, cadherins, immunoglobulin-cell adhesion molecules, and selectins. Pharmacol. Rev. 50 (2), 197–263.
Burnstock, G., 2009. Acupuncture: a novel hypothesis for the involvement of purinergic signalling. Med. Hypotheses 73, 470–472.
Chao, D.M., Shen, L.L, Tjen-A-Looi, S., Pitsillides, K.F., Li, P., Longhurst, J.C., 1999. Naloxone reverses inhibitory effect of electroacupuncture on sympathetic cardiovascular reflex responses. Am. J. Physiol. Jun. 276 (6 Pt 2), H2127–2134.
Cho, H., Shin, J., Shin, C.Y., Lee, S., Oh, U., 2002. Mechanosensitive ion channels in cultured sensory neurons of neonatal rats. J. Neurosci. 22 (4), 1238–1247.
Glantz, S.A., 2002. Primer of Biostatistics, 5th ed. McGraw-Hill, New York.
Gschossmann, J.M., Chaban, V.V., McRoberts, J.A., Raybould, H.E., Young, S.H., Ennes, H.S., Lembo, T., Mayer, E.A., 2000. Mechanical action of dorsal root ganglion cells in vitro: comparison with capsaicin and modulation by kappa-opioids. Brain Res. 856 (1–2), 101–110.
Kawada, T., Shimizu, S., Yamamoto, T., Shishido, T., Kamiya, A., Miyamoto, T., Sunagawa, K., Sugimachi, M., 2009. Servo-controlled hind-limb electrical stimulation for short-term arterial pressure control. Circ. J. 73 (5), 851–859.
Kimura, A., Sato, A., 1997. Somatic regulation of autonomic functions in anesthetized animals—neural mechanisms of physical therapy including acupuncture. Jpn J. Vet. Res. 45 (3), 137–145.
Langevin, H.M., Churchill, D.L., Cipolla, M.J., 2001. Mechanical signaling through connective tissue: a mechanism for the therapeutic effect of acupuncture. FASEB J. 15, 2275–2285.
Lin, M.C., Nahin, R., Gershwin, M.E., Longhurst, J.C., Wu, K.K., 2001. State of complementary and alternative medicine in cardiovascular, lung, and blood research: executive summary of a workshop. Circulation 103 (16), 2038–2041.
Nakamoto, T., Matsukawa, K., 2007. Muscle mechanosensitive receptors close to the myotendinous junction of the Achilles tendon elicit a pressor reflex. J. Appl. Physiol. 102, 2112–2120.
Napadow, V., Makris, N., Liu, J., Kettner, N.W., Kenneth, K.K., Hui, K.K.S., 2005. Effects of electroacupuncture versus manual acupuncture on the human brain as measured by fMRI. Hum. Brain Mapp. 24, 193–205.
Sato, A., Sato, Y., Schmidt, R.F., 1981. Heart rate changes reflecting modifications of efferent cardiac sympathetic outflow by cutaneous and muscle afferent volleys. J. Auton. Nerv. Syst. 4 (3), 231–247.
Sato, A., Sato, Y., Suzuki, A., Uchida, S., 1994. Reflex modulation of gastric and vesical function by acupuncture-like stimulation in anesthetized rats. Biomed. Res. 15, 59–65.
Sato, A., Sato, Y., Uchida, S., 2002. Reflex modulation of visceral functions by acupuncture-like stimulation in anesthetized rats. Int. Congr. Ser. 1238, 111–123.
Sator-Katzenschlager, S.M., Szeles, J.C., Scharbert, G., Michalek-Sauberer, A., Kober, A., Heinze, G., Kozek-Langenecker, S.A., 2003. Electrical stimulation of auricular acupuncture points is more effective than conventional manual auricular acupuncture in chronic cervical pain: a pilot study. Anesth. Analg. 97, 1469–1473.
Silberstein, M., 2009. The cutaneous intrinsic visceral afferent nervous system: a new model for acupuncture analgesia. J. Theor. Biol. 261, 637–642.
Tjen-A-Looi, S.C., Fu, L.-W., Zhou, W., Syuu, Z., Longhurst, J.C., 2005. Role of unmyelinated fibers in electroacupuncture cardiovascular responses. Auton. Neurosci. 118, 43–50.
Uchida, S., Shimura, M., Ohsawa, H., Suzuki, A., 2007. Neural mechanism of bradycardic responses elicited by acupuncture-like stimulation to a hind limb in anesthetized rats. J. Physiol. Sci. 57 (6), 377–382.
Uchida, S., Kagitani, F., Hotta, H., 2008. Mechanism of the reflex inhibition of heart rate elicited by acupuncture-like stimulation in anesthetized rats. Auton. Neurosci. 143, 12–19.
Wessberg, J., Olausson, H., Fernstrom, W.F., Vallbo, B.A., 2003. Receptive field properties of unmyelinated tactile afferents in the human skin. J. Neurophysiol. 89, 1567–1575.
Yamamoto, H., Kawada, T., Kamiya, A., Kita, T., Sugimachi, M., 2008. Electroacupuncture changes the relationship between cardiac and renal sympathetic nerve activities in anesthetized cats. Auton. Neurosci. 144 (1–2), 43–49.

Am J Physiol Regul Integr Comp Physiol 300: R969–R977, 2011.
First published January 26, 2011; doi:10.1152/ajpregu.00768.2010.

Exercise training augments the dynamic heart rate response to vagal but not sympathetic stimulation in rats

Masaki Mizuno,[1,2] Toru Kawada,[2] Atsunori Kamiya,[2] Tadayoshi Miyamoto,[2,3] Shuji Shimizu,[2] Toshiaki Shishido,[2] Scott A. Smith,[1] and Masaru Sugimachi[2]

[1]*Departments of Physical Therapy and Internal Medicine, University of Texas Southwestern Medical Center at Dallas, Dallas, Texas;* [2]*Department of Cardiovascular Dynamics, National Cerebral and Cardiovascular Center Research Institute, Osaka, Japan; and* [3]*Department of Physical Therapy, Morinomiya University of Medical Sciences, Osaka, Japan*

Submitted 23 November 2010; accepted in final form 26 January 2011

Mizuno M, Kawada T, Kamiya A, Miyamoto T, Shimizu S, Shishido T, Smith SA, Sugimachi M. Exercise training augments the dynamic heart rate response to vagal but not sympathetic stimulation in rats. *Am J Physiol Regul Integr Comp Physiol* 300: R969–R977, 2011. First published January 26, 2011; doi:10.1152/ajpregu.00768.2010.—We examined the transfer function of autonomic heart rate (HR) control in anesthetized sedentary and exercise-trained (16 wk, treadmill for 1 h, 5 times/wk at 15 m/min and 15-degree grade) rats for comparison to HR variability assessed in the conscious resting state. The transfer function from sympathetic stimulation to HR response was similar between groups (gain, 4.2 ± 1.5 vs. 4.5 ± 1.5 beats·min^{-1}·Hz^{-1}; natural frequency, 0.07 ± 0.01 vs. 0.08 ± 0.01 Hz; damping coefficient, 1.96 ± 0.55 vs. 1.69 ± 0.15; and lag time, 0.7 ± 0.1 vs. 0.6 ± 0.1 s; sedentary vs. exercise trained, respectively, means ± SD). The transfer gain from vagal stimulation to HR response was 6.1 ± 3.0 in the sedentary and 9.7 ± 5.1 beats·min^{-1}·Hz^{-1} in the exercise-trained group ($P = 0.06$). The corner frequency (0.11 ± 0.05 vs. 0.17 ± 0.09 Hz) and lag time (0.1 ± 0.1 vs. 0.2 ± 0.1 s) did not differ between groups. When the sympathetic transfer gain was averaged for very-low-frequency and low-frequency bands, no significant group effect was observed. In contrast, when the vagal transfer gain was averaged for very-low-frequency, low-frequency, and high-frequency bands, exercise training produced a significant group effect ($P < 0.05$ by two-way, repeated-measures ANOVA). These findings suggest that, in the frequency domain, exercise training augments the dynamic HR response to vagal stimulation but not sympathetic stimulation, regardless of the frequency bands.

heart rate variability; transfer function; systems analysis

HEART RATE VARIABILITY (HRV) is considered to be a useful noninvasive assessment of autonomic nervous system activity. It has been well recognized that exercise training increases HRV at rest (4, 19). A recent meta-analysis by Sandercock et al. (28) demonstrated that exercise training results in significant increases in R-R interval and high-frequency (HF) power of HRV. Nevertheless, not all studies have demonstrated increases in HRV after exercise training (7). To date, the exact mechanisms underlying increases in HRV after exercise training remain to be elucidated. Many earlier studies have suggested that the augmentation of HRV induced by exercise training may be caused by a withdrawal of sympathetic tonus and/or an increase in vagal tonus (5, 14, 36). Autonomic tone assessed by HRV may reflect both the autonomic outflow from the central nervous system and the peripheral autonomic regulation of atrial pacemaker cells. The latter can be assessed quantitatively by examining the heart rate (HR) response to electrical stimulation of the autonomic nerves. Furthermore, recent studies suggested that peripheral autonomic regulation of atrial pacemaker cells could contribute to the exercise training-induced increases in cardiac vagal function (9, 10).

Equivocal results, however, have been reported using autonomic nerve stimulation. Regarding the vagal system, the effects of exercise training have been inconsistent among studies, showing both increases (9, 10) and reductions in vagally stimulated HR control (25). When considering the sympathetic system, a previous study demonstrated that the HR response to sympathetic stimulation was reduced by exercise training (22). However, the mechanisms underlying the training effect are controversial (3, 15, 26, 29, 33, 35). These equivocal results could be explained by differences in species and modes of exercise training among studies (i.e., exercise type, intensity, and duration, etc.). More importantly, since these studies of autonomic nerve stimulation did not evaluate HRV, a causal relationship between increased HRV and adaptation in peripheral autonomic HR control remains largely undetermined. Furthermore, despite the fact that HRV has been evaluated by using frequency domain as well as time domain analyses, to date, there are no reports available examining the effects of exercise training on the dynamic HR response to sympathetic or vagal stimulation in the frequency domain. Analysis of peripheral autonomic regulation in the frequency domain would advance our understanding of the mechanisms responsible for the alterations in HRV that occur in response to exercise training.

We have recently developed a technique to assess the dynamic characteristics of HR control by the autonomic nervous system in rats using transfer function analysis (21). The transfer function analysis can quantitatively evaluate the HR response to autonomic nerve stimulation over a wide frequency range that is necessary for interpreting the generation of HRV. Therefore, the aims of the present study were *1*) to identify the dynamic characteristics of sympathetic and vagal HR control in exercised-trained rats and *2*) to determine whether alterations in peripheral autonomic regulation contribute to changes in the frequency components of HRV in exercised-trained rats.

MATERIALS AND METHODS

Animal Care and Training Program

Animal care was in accordance with the "Guiding Principles for Care and Use of Animals in the Field of Physiological Sciences," approved by the Physiological Society of Japan. All protocols were reviewed and approved by the Animal Subjects Committee of the

Address for reprint requests and other correspondence: M. Mizuno, Dept. of Physical Therapy, Univ. of Texas Southwestern Medical Center at Dallas, 5323 Harry Hines Blvd., Dallas, TX 75390-9174 (e-mail: masaki.mizuno@utsouthwestern.edu).

National Cerebral and Cardiovascular Center. Fourteen male Sprague-Dawley rats (200–250 g body wt) were fed standard laboratory chow and water ad libitum and housed three per cage in a temperature-controlled room with a 12:12-h dark-light cycle. Rats were randomly assigned to one of two groups: sedentary ($n = 7$) and exercise trained ($n = 7$).

Exercise training was performed on a motor-driven treadmill, 5 days/wk for 16 wk, gradually progressing toward a speed of 15 m/min at a 15-degree grade for 60 min. Sedentary rats walked (10 m/min at 15 degrees) 10 min/day once per week during the 16-wk period to maintain treadmill familiarity. At the end of the 16-wk period, maximal exercise capacity was measured twice in each rat in tests separated by 2 days (6). The protocol for the maximal exercise capacity test consisted of walking at 10 m/min for 5 min followed by 2 m/min increases in speed every 2 min until the rat reached exhaustion. Rats were considered exhausted when they failed to stay off of a shock bar.

Assessment of Autonomic Tone in the Conscious Resting State

After the performance test, three steel electrodes were implanted under anesthesia. These electrodes were utilized for monitoring the electrocardiogram. The R-R interval was measured using a cardiotachometer (model AT601G; Nihon Kohden, Tokyo, Japan). On the first day of the study, which was 24 h after electrodes had been implanted, resting HR was recorded to analyze the R-R interval variability in the quiet unrestrained rat that was kept in a small box. In accordance with a previous study (25), autonomic tone was assessed by intraperitoneal injections of methylatropine (3 mg/kg) and propranolol (4 mg/kg). Immediately after resting HR was recorded, methylatropine was injected. Since the HR response to methylatropine reached its peak in 10–15 min, this time interval was allocated before the HR measurement. Propranolol was injected after methylatropine injection, and again the HR was measured after 10–15 min. Intrinsic HR was evaluated after simultaneous blockade by propranolol and methylatropine. Sympathetic tonus was defined as the difference between the HR after methylatropine injection and intrinsic HR. On the second day, propranolol was administered first to obtain the inverse sequence of blockade. Vagal tonus was defined as the difference between the HR after propranolol injection and intrinsic HR.

Sympathetic and Vagal Stimulation

Surgical preparations. After obtaining data for the assessment of autonomic tone and HRV, rats were anesthetized by a mixture of urethane (250 mg/ml) and α-chloralose (40 mg/ml), initiated with an intraperitoneal bolus injection of 1 ml/kg. If additional anesthesia was needed, 0.1 ml/kg was given intraperitoneally. The rats were intubated and mechanically ventilated with oxygen-enriched room air. The rats were slightly hyperventilated to suppress chemoreflexes. A catheter was placed in the right femoral artery and connected to a pressure transducer (model DX-200; Nihon Kohden, Tokyo, Japan) to measure arterial pressure (AP). HR was measured using a cardiotachometer (model AT601G; Nihon Kohden) triggered by the R wave on the electrocardiogram. A catheter was introduced into the right femoral vein for drug administration. Sinoaortic barodenervation was performed bilaterally to minimize changes in sympathetic efferent nerve activity via arterial baroreflexes. The vagi were sectioned bilaterally at the neck. A pair of bipolar stainless steel electrodes was attached to the right cervical sympathetic nerve for efferent sympathetic stimulation or the right cervical vagus for efferent vagal stimulation. The stimulation electrodes and nerve were secured with silicon glue (Kwik-Sil; World Precision Instruments, Sarasota, FL). Body temperature was monitored with a thermometer placed in the rectum and was maintained at 38°C with a heating pad throughout the experiment.

Experimental procedures. The pulse duration was set at 2 ms and the stimulation amplitude was fixed at 10 V for both sympathetic and vagal nerve stimulation. To allow for stabilization of hemodynamics, sympathetic and vagal nerve stimulations were started ~1 h after the end of surgical preparations. Between sympathetic and vagal stimulation protocols > 15 min elapsed to allow AP and HR to return to their respective baseline values.

To estimate the dynamic transfer characteristics from sympathetic stimulation to HR response, the sectioned end of the right cervical sympathetic nerve was stimulated employing a frequency-modulated pulse train for 10 min. The stimulation frequency was switched every 1,000 ms to either 0 or 5 Hz according to a binary white noise signal. The power spectrum of the stimulation signal was reasonably constant up to 0.5 Hz. The transfer function was estimated up to 0.5 Hz because the reliability of estimation decreased due to the diminution of input power above this frequency. The selected frequency range sufficiently spanned the range of physiological interest (21). For estimation of the static transfer characteristics from sympathetic stimulation to HR response, stepwise sympathetic stimulation was performed. Sympathetic stimulation frequency was increased from 1 to 5 Hz in 1-Hz increments. Each frequency step was maintained for 60 s.

To estimate the dynamic transfer characteristics from vagal stimulation to HR response, the right vagus was stimulated employing a frequency-modulated pulse train for 10 min. The stimulation frequency was switched every 500 ms to either 0 or 10 Hz according to a binary white noise signal. The power spectrum of the stimulation signal was reasonably constant up to 1 Hz. The transfer function was estimated up to 1 Hz because the reliability of estimation decreased due to the diminution of input power above this frequency. The selected frequency range sufficiently spanned the range of physiological interest (21). For estimation of the static transfer characteristics from vagal stimulation to HR response, stepwise vagal stimulation was performed. Vagal stimulation frequency was changed among 2, 4, 8, 16, and 32 Hz. Each frequency step was maintained for 60 s.

Data Analysis

Spectral analysis of HRV. Data obtained during the conscious resting state were digitized at 200 Hz utilizing a 12-bit analog-to-digital converter and stored on the hard disk of a dedicated laboratory computer system. Beat-by-beat time series of the R-R interval were interpolated every 130 ms (Δt). Twelve data segments of 512 (N) points overlapping half of the preceding data were processed. For each data segment, after the linear trend was removed and the Hanning window applied, power spectral density was computed using the fast Fourier transform algorithm. The frequency resolution was $\Delta f = 1/(N\,\Delta t)$, i.e., 0.015 Hz, and the highest frequency was $\Delta f = 1/2\Delta t$, i.e., 3.85 Hz, where f is frequency. The very-low-frequency (VLF) band ranged between 0.017 and 0.27 Hz, the low-frequency (LF) band between 0.27 and 0.75 Hz, and the high-frequency (HF) band between 0.75 and 3.3 Hz, according to an earlier report (8). The percentage of LF or HF power relative to the sum of LF and HF powers and the ratio of LF to HF power were also calculated.

Transfer function analysis. The dynamic characteristics of the HR response to sympathetic or vagal stimulation were estimated by a transfer function analysis (see APPENDIX for details). Dynamic sympathetic control of HR was quantified by fitting a second-order low-pass filter with pure delay to the estimated transfer function. The dynamic vagal control of HR was quantified by fitting a first-order, low-pass filter with pure delay to the estimated transfer function. To facilitate the intuitive understanding of the system's dynamic characteristics, we calculated the system step response of HR to 1-Hz nerve stimulation as follows.

The system impulse response was derived from the inverse Fourier transform of the transfer function. The system step response was then obtained from the time integral of the impulse response. The length of the step response was 51.2 s. The 80% rise time for the sympathetic step response or the 80% fall time for the vagal step response was estimated as the time at which the step response reached 80% of the

Table 1. *Physical characteristics*

	Sedentary	Exercise Trained
Body weight, g	642 ± 33	534 ± 33*
Ventricular weight, g	1.22 ± 0.03	1.17 ± 0.04*
Ventricular weight/body weight, g/kg	1.9 ± 0.1	2.2 ± 0.1*
Lung weight, g	2.13 ± 0.27	1.89 ± 0.38
Lung weight/body weight, g/kg	3.3 ± 0.3	3.5 ± 0.7
Performance test, s	1150 ± 165	1790 ± 389*

Values are means ± SD. *$P < 0.05$ compared with sedentary group.

steady-state response calculated by averaging the last 10 s of data of the step response.

Statistical Analysis

All data are represented as means ± SD. Data were analyzed using unpaired Student's *t*-tests (sedentary vs. exercise trained) or two-way, repeated-measures ANOVA. Values of $P < 0.05$ were considered to be significant.

RESULTS

Physical Characteristic

Morphometric characteristics and exercise capacity for sedentary and exercised-trained rats are presented in Table 1. The mean body weight of the exercised-trained rats was significantly smaller than that of the sedentary rats. The mean ventricular weight of the exercised-trained rats was slightly but significantly smaller than that of the sedentary rats. Consequently, the ventricular weight normalized by body weight was significantly greater in the exercised-trained compared with the sedentary group. The lung weight-to-body weight ratio was not different between the groups. Exercise capacity was 64% greater in the exercised-trained than in the sedentary group. The reproducibility of measuring the maximal exercise capacity was reasonably high ($y = 1.2x - 226.1$, $R^2 = 0.79$; x and y represent the first and second measurements).

Spectral Analysis of HRV and Autonomic Tone in the Conscious Resting State

The power spectral densities of R-R interval are shown in Table 2. The percentage of LF power was significantly smaller, and the percentage of HF power was significantly greater in the exercised-trained rats than in the sedentary rats. The LF/HF ratio in the exercised-trained rats was significantly smaller compared with that in the sedentary rats. HR at rest was significantly lower in the exercised-trained compared with the sedentary group (Fig. 1*A*). The intrinsic HR was similar between the groups (Fig. 1*A*). Although the sympathetic tonus was comparable between the groups, the vagal tonus tended to be greater ($P = 0.08$) in the exercised-trained compared with the sedentary group (Fig. 1*B*).

Dynamic Sympathetic and Vagal Transfer Functions

Table 3 summarizes hemodynamics during dynamic sympathetic stimulation. Sympathetic stimulation significantly increased mean HR in both sedentary and exercised-trained groups. Mean HR and AP did not differ between the groups, before and during sympathetic stimulation. Figure 2*A* illustrates the dynamic transfer function characterizing sympathetic HR control. The frequency band effect was significant ($P < 0.0001$) but the group effect was insignificant ($P = 0.5461$) in the dynamic gain values of the sympathetic transfer function by two-way, repeated-measures ANOVA. The parameters of the sympathetic transfer function were comparable between the groups (Table 4). Figure 2*B* shows the calculated step response of HR to sympathetic stimulation. The steady-state response and the 80% rise time did not differ significantly between the groups (Table 4).

Table 5 summarizes hemodynamics during dynamic vagal stimulation. Vagal stimulation significantly decreased mean HR in both sedentary and exercised-trained groups. Mean HR and AP did not differ between the groups, before and during vagal stimulation. Figure 3*A* illustrates the dynamic transfer function characterizing vagal HR control. The frequency band effect ($P < 0.0001$) and the group effect ($P < 0.0001$) were both significant in the dynamic gain values of the vagal transfer function by two-way, repeated-measures ANOVA. The estimated dynamic gain (*see* APPENDIX) tended to be greater in the exercised-trained compared with the sedentary group ($P = 0.06$, Table 6). Other parameters did not differ between the groups. Figure 3*B* shows the calculated step response of HR to vagal stimulation. The calculated steady-state response in the exercised-trained rats also tended to be greater than that in the sedentary rats ($P = 0.06$, Table 6). There was no significant difference in the 80% fall time between the groups.

Dynamic Gain Values of Sympathetic and Vagal Transfer Function Corresponding to HRV Frequency Bands

When dynamic gain values of the sympathetic transfer function were averaged for the VLF and LF (up to 0.5 Hz, see METHODS) bands, the frequency band effect was significant, but the group effect was insignificant by two-way, repeated-measures ANOVA (Fig. 4*A*). When dynamic gain values of the vagal transfer function were averaged for the VLF, LF, and HF (up to 1 Hz, see METHODS) bands, the frequency band effect was insignificant but the group effect was significant such that the dynamic gain was significantly greater in the exercised-trained compared with the sedentary group (Fig. 4*B*).

Static Sympathetic and Vagal Transfer Function

The increase in HR with stepwise sympathetic stimulation was similar between groups (Fig. 5*A*). The stimulation frequency effect was significant, while the group effect was insignificant by two-way, repeated-measures ANOVA. In contrast, the decrease in HR with stepwise vagal stimulation was greater in the exercised-trained compared with sedentary rats (Fig. 5*B*). Both the stimulation frequency effect and the group effect were significant.

Table 2. *Spectral parameters of R-R interval*

	Sedentary	Exercise Trained
Variance, ms^2	87 ± 39	90 ± 32
VLF, ms^2	73 ± 30	80 ± 30
LF, ms^2	6.3 ± 3.4	3.1 ± 3.0
LF, %	49 ± 11	36 ± 7*
HF, ms^2	8.0 ± 7.6	6.2 ± 7.1
HF, %	51 ± 11	64 ± 7*
LF/HF ratio	1.0 ± 0.5	0.6 ± 0.2*

Values are means ± SD. LF, low frequency; VLF, very low frequency; HF, high frequency; *$P < 0.05$ compared with sedentary group.

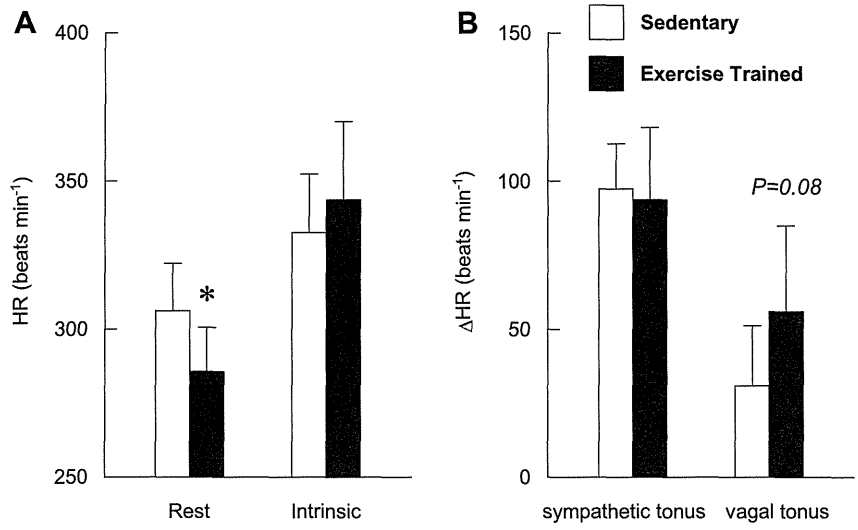

Fig. 1. Heart rate (HR) at rest and intrinsic HR (*A*) and HR sympathetic and vagal tone (*B*) obtained in sedentary and exercised-trained rats. *$P < 0.05$ compared with sedentary group.

DISCUSSION

We have examined the dynamic transfer function of autonomic HR control by using random binary sympathetic and vagal nerve stimulation in sedentary and exercised-trained rats. The major findings in the present study are *1*) that the exercise training did not alter the sympathetic transfer function substantially but augmented the dynamic gain of the vagal transfer function; and *2*) in the frequency domain, exercise training increased the dynamic HR response to vagal stimulation but not sympathetic stimulation, regardless of the frequency band. These findings are the first quantitative data on the effect of exercise training on the dynamic characteristics of peripheral HR control by the sympathetic and vagal systems.

Validity of Exercise Training

The relative ventricular hypertrophy and higher exercise capacity in the exercised-trained compared with the sedentary group suggested that exercise program used in the present study was sufficient to induce physiological adaptations commensurate with an effective training stimulus. As is well known, exercise training induces bradycardia at rest (Fig. 1*A*). Moreover, changes in the spectral parameters for R-R interval (Table 2) and autonomic tone (Fig. 1*B*) induced by the exercise training are consistent with earlier studies in rats (30, 31).

Effect of Exercise Training on Sympathetic and Vagal Transfer Function

Exercise training altered neither dynamic (Fig. 2) nor static sympathetic transfer function (Fig. 5*A*). These results are different than those reported in a previous study in which swim training significantly reduced the HR response to sympathetic nerve stimulation in a double atrial/right stellate ganglion preparation in guinea pigs (22). The discrepancy between investigations may have arisen from differences in the nerves experimentally stimulated (cervical sympathetic nerve vs. stellate ganglion), animal species studied (rats vs. guinea pigs), and/or experimental preparation utilized (in vivo vs. ex vivo). The mechanisms underlying the sympathetically mediated exercise training effect on HR are also controversial. For instance, chronotropic responsiveness to isoproterenol has been reported to be decreased in one study (15) but unchanged in another (22) by exercise training. Furthermore, in response to exercise training, the density and affinity of β-adrenoceptors in the heart have been shown to be reduced in some reports (26, 33), while unchanged in others (3, 34, 35).

Table 3. *Arterial pressure(AP) and heart rate (HR) during dynamic sympathetic stimulation protocol*

	Sedentary		Exercise Trained	
	Prestimulation	During Stimulation	Prestimulation	During Stimulation
AP, mmHg	74 ± 16	68 ± 15†	89 ± 17	84 ± 24
HR, beats/min	377 ± 25	444 ± 23†	381 ± 16	444 ± 26†

Values are means ± SD. †$P < 0.05$ compared with prestimulation.

Exercise training augmented the dynamic gain of the vagal transfer function (Fig. 2). The effect of exercise training was also significant for static vagal transfer function (Fig. 5*B*). These results are in agreement with previous studies showing that exercise training significantly augmented the HR response to vagal nerve stimulation in a double atrial/right vagal nerve preparation using mice (9, 10). In contrast, Negrao et al. (25) demonstrated that the HR response to vagal stimulation was depressed in exercised-trained rats. A possible explanation for this disparate result is that the arterial baroreflexes remained intact in the experimental preparation used in the study (25). In contrast, sinoaortic barodenervation was performed in the present investigation to minimize baroreflex-mediated changes in sympathetic efferent nerve activity. Exercise training has been shown to attenuate the baroreflex-mediated sympathetic nerve response to hypotension (11). Although speculative, in the study by Negrao et al. (25), baroreflex-mediated sympathetic activation in response to vagally-induced hypotension might have been less in exercised-trained compared with sedentary rats. Consequently, the gain of vagal stimulation might have been attenuated in exercised-trained animals relative to sedentary rats. This suggestion is reasonable given that accentuated antagonism is indicative of a diminution in background sym-

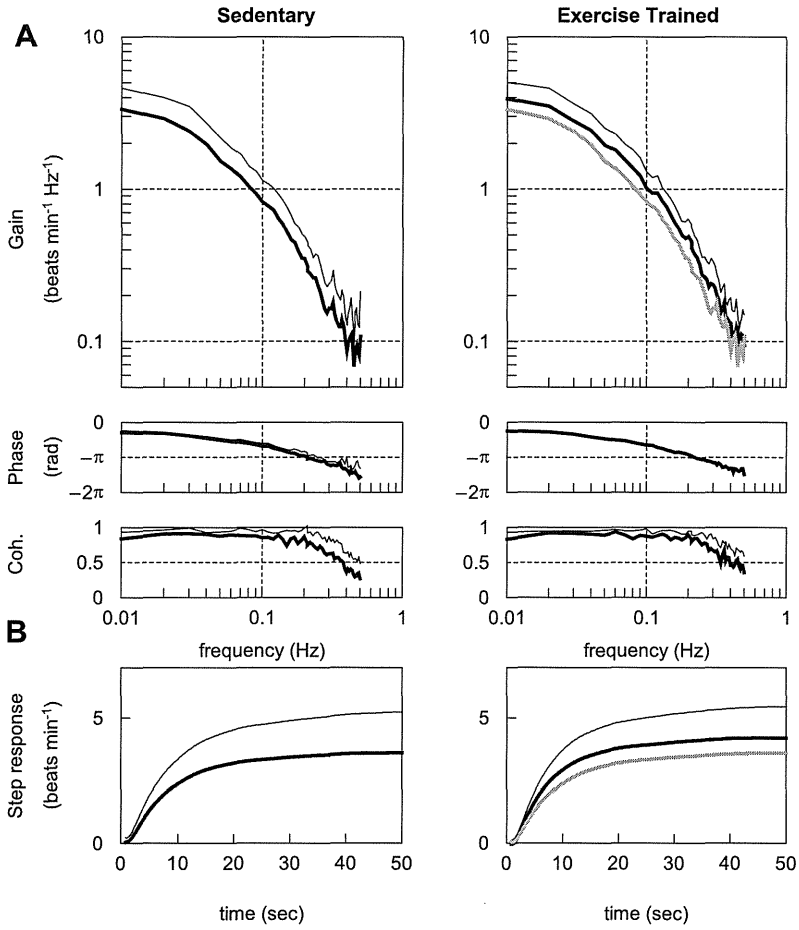

Fig. 2. *A*: transfer function from sympathetic stimulation to the HR response obtained in sedentary and exercised-trained rats. Gains (*top*), phase shifts (*middle*), and coherence (Coh.) functions (*bottom*) are presented. *B*: calculated step response to 1-Hz tonic sympathetic stimulation. Thick lines represent the mean, whereas thin lines indicate ± SD values. The gray solid curves in the gain and step response panels (*right*) duplicates the means (*left*).

pathetic tonus, which can decrease the gain of the vagal transfer function (17).

It has been documented that the intensity of exercise as well as the duration of exercise training are related to the autonomic adaptation to exercise training (28). These factors have been shown to be largely variable among different studies. A well-controlled experimental setup is needed to clarify these issues.

Dynamic Gain Values of Sympathetic and Vagal Transfer Functions Corresponding to HRV Frequency Bands

HRV is considered to reflect autonomic tone (19). The VLF component is likely to reflect changes in vasomotor tone in relation to thermoregulation and local adjustment of resistance in individual vascular beds; the LF component is considered to be a marker of sympathetic activity, although it remains a matter of debate; and the HF component mainly originates from respiratory activity and is considered to be mediated by vagal input (27). In rats, Cerutti et al. (8) determined that the LF component ranged between 0.27 and 0.74 Hz, and the HF component was > 0.75 Hz.

Averaged dynamic gain values of sympathetic transfer function for VLF and LF bands did not differ between the sedentary and exercised-trained groups (Fig. 4*A*). These results suggest that changes in the peripheral sympathetic control of HR likely do not contribute significantly to training-induced alterations in HRV. Therefore, the lower percentage of LF power and LF/HF ratio in the exercised-trained group (Table 2) may indicate reduced activation of sympathetic outflow from autonomic centers (23). In contrast, averaged dynamic gain values of vagal transfer function for VLF, LF, and HF bands (Fig. 4*B*) as

Table 4. *Sympathetic transfer function parameters and step response*

	Sedentary	Exercise Trained
Gain, beats·min^{-1}·Hz^{-1}	4.2 ± 1.5	4.5 ± 1.5
Natural frequency, Hz	0.07 ± 0.01	0.08 ± 0.01
Damping ratio	1.96 ± 0.55	1.69 ± 0.15
Lag time, s	0.71 ± 0.10	0.62 ± 0.11
Steady-state response, beats/min	3.6 ± 1.6	4.2 ± 1.2
80% rise time, s	12.9 ± 2.7	12.1 ± 3.0

Values are means ± SD. See APPENDIX for transfer function parameters.

Table 5. *AP and HR during dynamic vagal stimulation protocol*

	Sedentary		Exercise Trained	
	Prestimulation	During stimulation	Prestimulation	During stimulation
AP, mmHg	72 ± 21	68 ± 15	92 ± 14	80 ± 21
HR, beats/min	373 ± 18	327 ± 38 †	372 ± 14	301 ± 32 †

Values are means ± SD. †$P < 0.05$ compared with prestimulation.

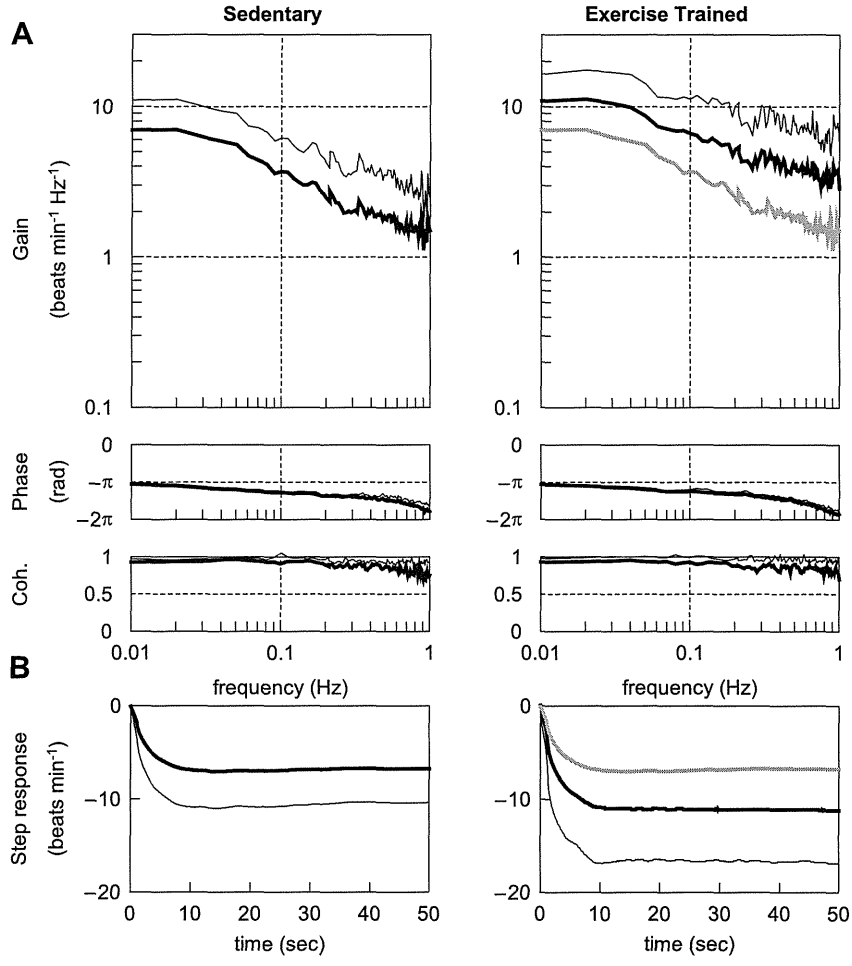

Fig. 3. *A*: transfer function from vagal stimulation to the HR response obtained in sedentary and exercised-trained rats. Gains (*top*), phase shifts (*middle*), and coherence functions (*bottom*) are presented. *B*: calculated step response to 1-Hz tonic vagal stimulation. Thick lines represent the mean, whereas thin lines indicate ± SD values. The gray solid curves in the gain and step response panels (*right*) duplicate the means (*left*).

well as the percentage of HF power (Table 2) were significantly greater in the exercised-trained compared with the sedentary group. These results suggest that the augmentation in HRV induced by exercise training is, at least in part, mediated by augmentations in the peripheral vagal control of HR.

What are the possible mechanisms underlying augmentations in the peripheral vagal control of HR? Danson and Paterson (10) have presented evidence that neuronal nitric oxide synthase may be a key enzymatic protein underlying such training-induced increases in cardiac vagal function. This group has also demonstrated that HR changes in response to vagal stimulation are enhanced by exercise training in wild-type mice but not in heterozygous neuronal nitric oxide synthase knockout mice (9). Another candidate for augmentations in the peripheral vagal control of HR is muscarinic receptors, which play a fundamental role in HR control via vagally mediated regulation. However, the effects of exercise training have been inconsistent among studies, showing both increases (12) and no change (2, 3) in muscarinic receptors in the myocardium of rats. The possibility cannot be dismissed that training-induced changes in the activity of afferent inputs mediating vagal outflow may also contribute to the alterations in HRV (4). Further investigation is needed to clarify these issues.

Table 6. *Vagal transfer function parameters and step response*

	Sedentary	Exercise Trained
Gain, beats·min^{-1}·Hz^{-1}	6.1 ± 3.0	9.7 ± 5.1#
Corner frequency, Hz	0.11 ± 0.05	0.17 ± 0.09
Lag time, s	0.10 ± 0.08	0.17 ± 0.08
Steady-state response, beats/min	−6.7 ± 3.6	−11.2 ± 5.7#
80% Fall time, s	4.3 ± 2.2	4.3 ± 1.5

Values are means ± SD. #P = 0.06 compared with sedentary group. See APPENDIX for transfer function parameters.

Perspectives and Significance

To date, the mechanisms underlying increased HRV after exercise training remain to be elucidated. HRV may reflect both the autonomic outflow from the central nervous system and the peripheral autonomic regulation of atrial pacemaker cells. In human studies, it is difficult to separately examine each factor. The findings of the present study suggest that the augmentation in HRV induced by exercise training is, at least in part, mediated by augmentations in the peripheral vagal control of HR. In other words, even if vagal outflow from the central nervous system remains unchanged after exercise training, HRV could be increased by an enhanced responsiveness in the peripheral vagal, but not sympathetic, regulation of HR.

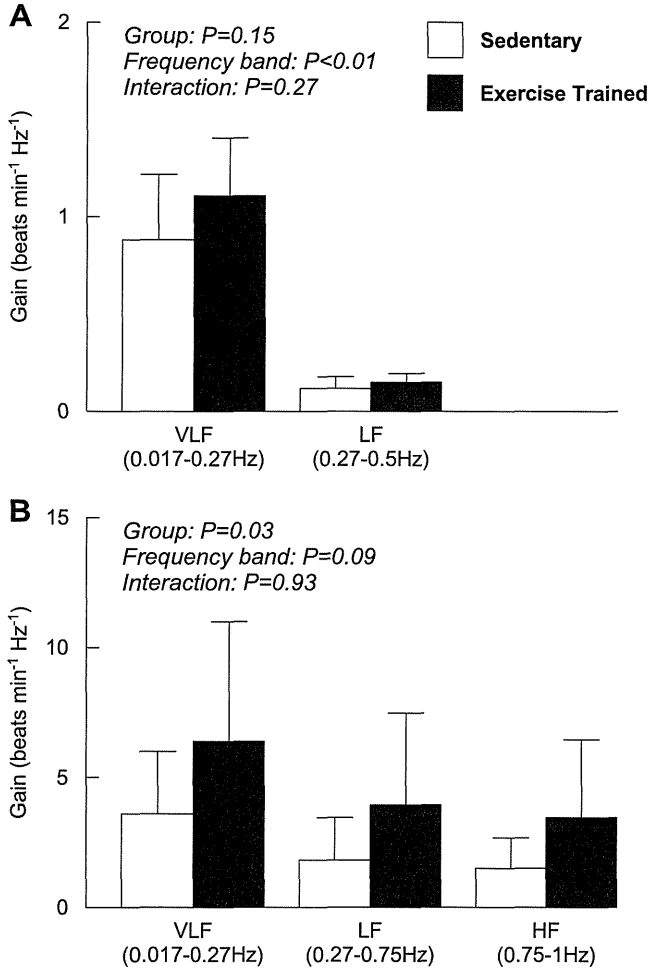

Fig. 4. Averaged sympathetic (*A*) and vagal (*B*) gain calculated from corresponding transfer function in very low frequency (VLF), low frequency (LF), and high frequency (HF) bands.

It has been well documented that decreased HRV is observed in heart failure (18) as well as in a variety of lifestyle-related diseases such as diabetes (16), hypertension (24), and obesity (1). Furthermore, reductions in HRV are related to increases in mortality rates as well as the occurrence of adverse cardiac events (32). Exercise training-induced augmentations in HRV maintain the potential to partially correct or normalize the autonomic dysfunction manifest in these disease states (4). Understanding the mechanisms contributing to the alterations in HRV induced by exercise training may significantly impact the development of novel therapeutic strategies for the treatment of autonomic dysfunction.

Limitations

There are several limitations to this study. First, the rats were slightly hyperventilated throughout the stimulation protocol. We cannot rule out the possibility that the hyperventilation might have affected the results reported. Second, dynamic sympathetic stimulation lowered mean AP in sedentary rats although sinoaortic barodenervation was performed. This may be explained by a possible difference in left ventricular functional capacity. For example, under conditions of equivalent HR, changes in systolic blood pressure were smaller in sedentary rats compared with exercised-trained rats (13). Third, the stimulation amplitude was fixed at 10 V for both sympathetic and vagal nerve stimulation. It should be noted, however, that our preliminary results indicated that 10 V was sufficiently large enough to evoke maximal HR responses. Fourth, transfer function data were obtained from anesthetized animals. This must be taken into account when interpreting the present results as anesthesia may affect the peripheral autonomic regulation of atrial pacemaker cells. Finally, we stimulated the sympathetic and vagal nerves according to a binary white noise signal. Although this method of stimulation is quite different from the physiological pattern of neuronal discharge, the coherence was near unity over the frequency range of interest. This finding indicates that the system properties do not vary considerably in response to different patterns of stimulation.

Conclusion

In the present study, it was demonstrated for the first time that exercise training did not alter dynamic sympathetic control of HR, while it did augment dynamic vagal control of HR. In addition, the group effect was significant with regard to the dynamic gain values for the vagal transfer functions corresponding to VLF, LF, and HF bands. This finding suggests that enhancements in the peripheral vagal control of HR may, at

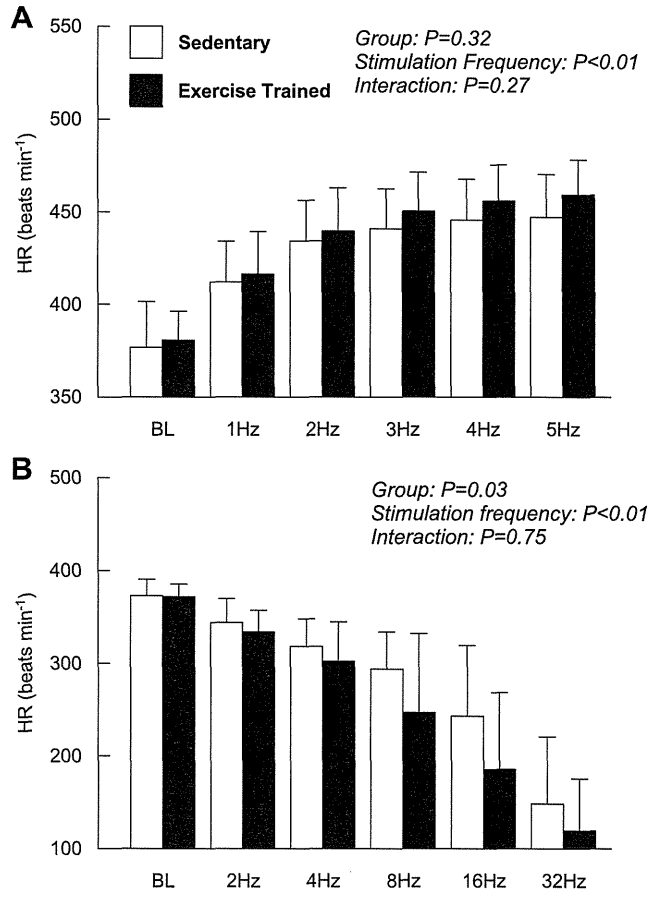

Fig. 5. HR response to stepwise sympathetic (*A*) and vagal (*B*) stimulation obtained in sedentary and exercised-trained rats.

least in part, contribute to the exercise-induced augmentation in HRV in healthy rats.

APPENDIX: TRANSFER FUNCTION ANALYSIS

The dynamic transfer function from binary white noise stimulation to the HR response was estimated based on the following procedure. Input-output data pairs of the stimulation frequency and HR were resampled at 10 Hz to be consistent with our previous study (21). Subsequently, data pairs were partitioned into eight 50% overlapping segments consisting of 1,024 data points each. For each segment, the linear trend was subtracted and a Hanning window was applied. A fast Fourier transform was then performed to obtain the frequency spectra of nerve stimulation [$N(f)$] and HR [$HR(f)$]. Over the eight segments, the power of the nerve stimulation [$S_{N\cdot N}(f)$], the power of the HR [$S_{HR\cdot HR}(f)$], and the cross-power between these two signals [$S_{N\cdot HR}(f)$] were ensemble averaged. Finally, the transfer function [$H(f)$] from nerve stimulation to the HR response was determined using the following equation (20).

$$H(f) = \frac{S_{N\text{-}HR}(f)}{S_{N\cdot N}(f)}$$

To quantify the linear dependence of the HR response on vagal or sympathetic stimulation, the magnitude-squared coherence function [$\mathrm{Coh}(f)$] was estimated employing the following equation (20).

$$\mathrm{Coh}(f) = \frac{|S_{\mathrm{N\text{-}HR}}(f)|^2}{S_{\mathrm{N\cdot N}}(f) \cdot S_{\mathrm{HR\cdot HR}}(f)}$$

Coherence values range from zero to unity. Unity coherence indicates perfect linear dependence between the input and output signals; in contrast, zero coherence indicates total independence between the two signals.

Since the transfer function from sympathetic stimulation to HR response in rats approximated a second order low-pass filter with pure delay (21), we determined the parameters of the sympathetic transfer function using the following equation.

$$H(f) = \frac{K}{1 + 2\zeta\frac{f}{f_N}j + \left(\frac{f}{f_N}j\right)^2} e^{-2\pi f j L}$$

where K is dynamic gain (in beats·min^{-1}·Hz^{-1}), f_N is the natural frequency (in Hz), ζ is the damping ratio, L is lag time (in s), and f and j represent frequency and imaginary units, respectively. These parameters were estimated by means of an iterative nonlinear least squares regression.

Since the transfer function from vagal stimulation to HR response in rats approximated a first-order, low-pass filter with pure delay (21), we determined the parameters of the vagal transfer function using the following equation.

$$H(f) = \frac{-K}{1 + \frac{f}{f_C}j} e^{-2\pi f j L}$$

where K represents the dynamic gain (in beats·min^{-1}·Hz^{-1}), f_C denotes the corner frequency (in Hz), L denotes the lag time (in s), and f and j represent frequency and imaginary units, respectively. The negative sign in the numerator indicates the negative HR response to vagal stimulation. These parameters were estimated by means of an iterative nonlinear least squares regression.

GRANTS

This study was supported by Health and Labor Sciences Research Grants H18-nano-Ippan-003, H19-nano-Ippan-009, H20-katsudo-Shitei-007, and H21-nano-Ippan-005 from the Ministry of Health, Labor and Welfare of Japan, by Grants-in-Aid for Scientific Research No. 19700559 from the Ministry of Education, Culture, Sports, Science and Technology in Japan, and by the Industrial Technology Research Grant Program from New Energy and Industrial Technology Development Organization of Japan. M. Mizuno was supported from Research Fellowships of the Japan Society for the Promotion of Science for Young Scientists.

DISCLOSURES

No conflicts of interest, financial or otherwise, are declared by the author(s).

REFERENCES

1. **Arone LJ, Mackintosh R, Rosenbaum M, Leibel RL, Hirsch J.** Autonomic nervous system activity in weight gain and weight loss. *Am J Physiol Regul Integr Comp Physiol* 269: R222–R225, 1995.
2. **Barbier J, Rannou-Bekono F, Marchais J, Berthon PM, Delamarche P, Carre F.** Effect of training on β1-, β2-, β3-adrenergic and M2 muscarinic receptors in rat heart. *Med Sci Sports Exerc* 36: 949–954, 2004.
3. **Barbier J, Reland S, Ville N, Rannou-Bekono F, Wong S, Carre F.** The effects of exercise training on myocardial adrenergic and muscarinic receptors. *Clin Auton Res* 16: 61–65, 2006.
4. **Billman GE.** Cardiac autonomic neural remodeling and susceptibility to sudden cardiac death: effect of endurance exercise training. *Am J Physiol Heart Circ Physiol* 297: H1171–H1193, 2009.
5. **Blomqvist CG, Saltin B.** Cardiovascular adaptations to physical training. *Annu Rev Physiol* 45: 169–189, 1983.
6. **Brenner DA, Apstein CS, Saupe KW.** Exercise training attenuates age-associated diastolic dysfunction in rats. *Circulation* 104: 221–226, 2001.
7. **Buch AN, Coote JH, Townend JN.** Mortality, cardiac vagal control and physical training–what's the link? *Exp Physiol* 87: 423–435, 2002.
8. **Cerutti C, Gustin MP, Paultre CZ, Lo M, Julien C, Vincent M, Sassard J.** Autonomic nervous system and cardiovascular variability in rats: a spectral analysis approach. *Am J Physiol Heart Circ Physiol* 261: H1292–H1299, 1991.
9. **Danson EJ, Mankia KS, Golding S, Dawson T, Everatt L, Cai S, Channon KM, Paterson DJ.** Impaired regulation of neuronal nitric oxide synthase and heart rate during exercise in mice lacking one nNOS allele. *J Physiol* 558: 963–974, 2004.
10. **Danson EJ, Paterson DJ.** Enhanced neuronal nitric oxide synthase expression is central to cardiac vagal phenotype in exercise-trained mice. *J Physiol* 546: 225–232, 2003.
11. **DiCarlo SE, Bishop VS.** Exercise training attenuates baroreflex regulation of nerve activity in rabbits. *Am J Physiol Heart Circ Physiol* 255: H974–H979, 1988.
12. **Favret F, Henderson KK, Clancy RL, Richalet JP, Gonzalez NC.** Exercise training alters the effect of chronic hypoxia on myocardial adrenergic and muscarinic receptor number. *J Appl Physiol* 91: 1283–1288, 2001.
13. **Fitzsimons DP, Bodell PW, Herrick RE, Baldwin KM.** Left ventricular functional capacity in the endurance-trained rodent. *J Appl Physiol* 69: 305–312, 1990.
14. **Goldsmith RL, Bigger JT Jr, Steinman RC, Fleiss JL.** Comparison of 24-hour parasympathetic activity in endurance-trained and untrained young men. *J Am Coll Cardiol* 20: 552–558, 1992.
15. **Hammond HK, White FC, Brunton LL, Longhurst JC.** Association of decreased myocardial β-receptors and chronotropic response to isoproterenol and exercise in pigs following chronic dynamic exercise. *Circ Res* 60: 720–726, 1987.
16. **Ikeda T, Matsubara T, Sato Y, Sakamoto N.** Circadian blood pressure variation in diabetic patients with autonomic neuropathy. *J Hypertens* 11: 581–587, 1993.
17. **Kawada T, Ikeda Y, Sugimachi M, Shishido T, Kawaguchi O, Yamazaki T, Alexander J Jr, Sunagawa K.** Bidirectional augmentation of heart rate regulation by autonomic nervous system in rabbits. *Am J Physiol Heart Circ Physiol* 271: H288–H295, 1996.
18. **La Rovere MT, Pinna GD, Maestri R, Mortara A, Capomolla S, Febo O, Ferrari R, Franchini M, Gnemmi M, Opasich C, Riccardi PG, Traversi E, Cobelli F.** Short-term heart rate variability strongly predicts sudden cardiac death in chronic heart failure patients. *Circulation* 107: 565–570, 2003.

19. **Malliani A, Pagani M, Lombardi F, Cerutti S.** Cardiovascular neural regulation explored in the frequency domain. *Circulation* 84: 482–492, 1991.
20. **Marmarelis P, Marmarelis V.** The white noise method in system identification. In: *Analysis of Physiological Systems*. New York: Plenum, 1978, p. 131–221.
21. **Mizuno M, Kawada T, Kamiya A, Miyamoto T, Shimizu S, Shishido T, Smith SA, Sugimachi M.** Dynamic characteristics of heart rate control by the autonomic nervous system in rats. *Exp Physiol* 95: 919–925, 2010.
22. **Mohan RM, Choate JK, Golding S, Herring N, Casadei B, Paterson DJ.** Peripheral pre-synaptic pathway reduces the heart rate response to sympathetic activation following exercise training: role of NO. *Cardiovasc Res* 47: 90–98, 2000.
23. **Mueller PJ.** Exercise training attenuates increases in lumbar sympathetic nerve activity produced by stimulation of the rostral ventrolateral medulla. *J Appl Physiol* 102: 803–813, 2007.
24. **Mussalo H, Vanninen E, Ikaheimo R, Laitinen T, Laakso M, Lansimies E, Hartikainen J.** Heart rate variability and its determinants in patients with severe or mild essential hypertension. *Clin Physiol* 21: 594–604, 2001.
25. **Negrao CE, Moreira ED, Santos MC, Farah VM, Krieger EM.** Vagal function impairment after exercise training. *J Appl Physiol* 72: 1749–1753, 1992.
26. **Nieto JL, Laviada ID, Guillen A, Haro A.** Adenylyl cyclase system is affected differently by endurance physical training in heart and adipose tissue. *Biochem Pharmacol* 51: 1321–1329, 1996.
27. **Pagani M, Lombardi F, Guzzetti S, Rimoldi O, Furlan R, Pizzinelli P, Sandrone G, Malfatto G, Dell'Orto S, Piccaluga E.** Power spectral analysis of heart rate and arterial pressure variabilities as a marker of sympatho-vagal interaction in man and conscious dog. *Circ Res* 59: 178–193, 1986.
28. **Sandercock GR, Bromley PD, Brodie DA.** Effects of exercise on heart rate variability: inferences from meta-analysis. *Med Sci Sports Exerc* 37: 433–439, 2005.
29. **Schwarz P, Diem R, Dun NJ, Forstermann U.** Endogenous and exogenous nitric oxide inhibits norepinephrine release from rat heart sympathetic nerves. *Circ Res* 77: 841–848, 1995.
30. **Souza SB, Flues K, Paulini J, Mostarda C, Rodrigues B, Souza LE, Irigoyen MC, De Angelis K.** Role of exercise training in cardiovascular autonomic dysfunction and mortality in diabetic ovariectomized rats. *Hypertension* 50: 786–791, 2007.
31. **Tezini GC, Silveira LC, Villa-Cle PG Jr, Jacinto CP, Di Sacco TH, Souza HC.** The effect of aerobic physical training on cardiac autonomic control of rats submitted to ovariectomy. *Menopause* 16: 110–116, 2009.
32. **Tsuji H, Larson MG, Venditti FJ Jr, Manders ES, Evans JC, Feldman CL, Levy D.** Impact of reduced heart rate variability on risk for cardiac events. The Framingham Heart Study. *Circulation* 94: 2850–2855, 1996.
33. **Werle EO, Strobel G, Weicker H.** Decrease in rat cardiac β1- and β2-adrenoceptors by training and endurance exercise. *Life Sci* 46: 9–17, 1990.
34. **Williams RS.** Physical conditioning and membrane receptors for cardioregulatory hormones. *Cardiovasc Res* 14: 177–182, 1980.
35. **Williams RS, Schaible TF, Bishop T, Morey M.** Effects of endurance training on cholinergic and adrenergic receptors of rat heart. *J Mol Cell Cardiol* 16: 395–403, 1984.
36. **Yamamoto K, Miyachi M, Saitoh T, Yoshioka A, Onodera S.** Effects of endurance training on resting and post-exercise cardiac autonomic control. *Med Sci Sports Exerc* 33: 1496–1502, 2001.

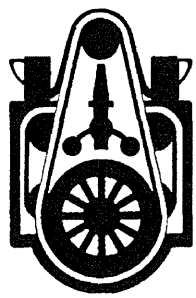

Am J Physiol Heart Circ Physiol 298: H1966–H1975, 2010.
First published March 26, 2010; doi:10.1152/ajpheart.00340.2009.

Parallel resetting of arterial baroreflex control of renal and cardiac sympathetic nerve activities during upright tilt in rabbits

Atsunori Kamiya, Toru Kawada, Masaki Mizuno, Shuji Shimizu, and Masaru Sugimachi
Department of Cardiovascular Dynamics, National Cardiovascular Centre Research Institute, Suita, Japan

Submitted 8 April 2009; accepted in final form 23 March 2010

Kamiya A, Kawada T, Mizuno M, Shimizu S, Sugimachi M. Parallel resetting of arterial baroreflex control of renal and cardiac sympathetic nerve activities during upright tilt in rabbits. *Am J Physiol Heart Circ Physiol* 298: H1966–H1975, 2010. First published March 26, 2010; doi:10.1152/ajpheart.00340.2009.—Since humans are under ceaseless orthostatic stress, the mechanisms to maintain arterial pressure (AP) against gravitational fluid shift are important. As one mechanism, it was reported that upright tilt reset baroreflex control of renal sympathetic nerve activity (SNA) to a higher SNA in anesthetized rabbits. In the present study, we tested the hypothesis that upright tilt causes a parallel resetting of baroreflex control of renal and cardiac SNAs in anesthetized rabbits. In anesthetized rabbits (n = 8, vagotomized and aortic denervated) with 0° supine and 60° upright tilt postures, renal and cardiac SNAs were simultaneously recorded while isolated intracarotid sinus pressure (CSP) was increased stepwise from 40 to 160 mmHg with increments of 20 mmHg. Upright tilt shifted the reverse-sigmoidal curve of the CSP-SNA relationship to higher SNA similarly in renal and cardiac SNAs. Although upright tilt increased the maximal gain, the response range and the minimum value of SNA, the curves were almost superimposable in these SNAs regardless of postures. Scatter plotting of cardiac SNA over renal SNA during the stepwise changes in CSP was close to the line of identity in 0° supine and 60° upright tilt postures. In addition, upright tilt also shifted the reverse-sigmoidal curve of the CSP-heart rate relationship to a higher heart rate, with increases in the maximal gain and the response range. In conclusion, upright posture caused a resetting of arterial baroreflex control of SNA similarly in renal and cardiac SNAs in anesthetized rabbits.

blood pressure; orthostasis; sympathetic nervous system

SINCE HUMANS ARE UNDER CEASELESS orthostatic stress, the mechanisms to maintain arterial pressure (AP) against gravitational fluid shift are greatly important. During standing, a gravitational fluid shift directed toward the lower part of the body (such as the abdominal vascular bed and lower limbs) will cause severe postural hypotension if not counteracted by compensatory mechanisms (15). Arterial baroreflexes have been considered to be the major compensatory mechanism (1, 13, 15), since denervation of baroreceptor afferents causes profound postural hypotension (16). In addition, we (8) recently reported that upright tilt resets baroreflex control of sympathetic nerve activity (SNA) to higher SNA. The resetting doubles SNA, compensates for the reduced pressor responses of cardiovascular organs to SNA during gravitational stress, and contributes to prevent postural hypotension. However, since the study recorded only renal SNA, it remains unknown whether upright tilt resets arterial baroreflex control of SNA innervating cardiovascular organs (i.e., the heart) other than the kidney. Since cardiac SNA has a critical role in circulation, baroreflex control of cardiac SNA during orthostatic stress is of importance.

Accordingly, in the present study, we tested the hypothesis that upright tilt causes a parallel resetting of arterial baroreflex control of renal and cardiac SNAs in anesthetized rabbits. Since total baroreflex is a closed-loop negative feedback system that senses baroreceptor pressure and controls AP, and since the baroreflex control of SNA (from baroreceptor pressure input to SNA) is a subsystem of the total baroreflex system, it is difficult to isolate the baroreflex control of SNA from the total system in the baroreflex closed-loop condition (16). Therefore, we opened the baroreflex feedback loop by vascularly isolating the carotid sinus region and loaded artificial stepwise intracarotid sinus pressure (CSP) in anesthetized rabbits. By recording renal and cardiac SNAs simultaneously, we investigated static characteristics of baroreflex control of these SNAs (CSP-SNA relationship) in 0° and 60° upright tilt postures.

METHODS

Animals, preparation, and measurements. Japanese White rabbits weighing 2.4–3.3 kg were used. Animals were cared for in strict accordance with the "Guiding Principles for the Care and Use of Animals in the Field of Physiological Science" approved by the Physiological Society of Japan.

Animals (n = 8) were initially anesthetized by intravenous injection (2 ml/kg) of a mixture of urethane (250 mg/ml) and α-chloralose (40 mg/ml). Anesthesia was maintained by continuously infusing the anesthetics at a rate of 0.33 $ml \cdot kg^{-1} \cdot h^{-1}$ using a syringe pump (CFV-3200; Nihon Kohden, Tokyo, Japan). The rabbits were mechanically ventilated with oxygen-enriched room air. Bilateral carotid sinuses were isolated vascularly from the systemic circulation by ligating the internal and external carotid arteries and other small branches originating from the carotid sinus regions. The isolated carotid sinuses were filled with warmed physiological saline, preequilibrated with atmospheric air, through catheters inserted via the common carotid arteries. The intracarotid sinus pressure (CSP) was controlled by a servo-controlled piston pump (model ET-126A; Labworks, Costa Mesa, CA). Bilateral vagal and aortic depressor nerves were sectioned in the middle of the neck region to eliminate reflexes from the cardiopulmonary region and the aortic arch. The systemic AP was measured using a high-fidelity pressure transducer (Millar Instruments, Houston, TX) inserted retrograde from the right common carotid artery below the isolated carotid sinus region. Heart rate (HR) was measured with a cardiotachometer (model N4778; San-ei, Tokyo, Japan).

Body temperature was maintained at around 38°C with a heating pad. The left renal sympathetic nerve was exposed retroperitoneally, and the left cardiac sympathetic nerve was exposed through a middle thoracotomy. A pair of stainless steel wire electrodes (Bioflex wire AS633; Cooner Wire) was hooked onto each of these nerves to record renal and cardiac SNAs. The nerve fibers peripheral to electrodes were ligated securely and crushed to eliminate afferent signals. The nerve

Address for reprint requests and other correspondence: A. Kamiya, Dept. of Cardiovascular Dynamics, National Cardiovascular Centre Research Institute, Suita 565-8565, Japan (e-mail: kamiya@ri.ncvc.go.jp).

and electrodes were covered with a mixture of silicone gel (silicon low viscosity, Kwik-Sil; World Precision Instruments, Sarasota, FL) to insulate and immobilize the electrodes. The preamplified SNA signals were band-pass filtered at 150–1,000 Hz. These nerve signals were full-wave rectified and low-pass filtered with a cutoff frequency of 30 Hz to quantify the nerve activity. After the experiment, an intravenous infusion of hexamethonium bromide (6 mg/kg) abolished the SNA signals, indicating that the signals recorded were postganglionic SNA.

Protocols. After the preparation, the animal was maintained in a 0° supine posture on a tilt bed. To stabilize the posture, the head was fixed full-frontal to the bed by strings, and the body and legs were rigged up in a clothes-like bag. Bilateral CSP was artificially controlled independently of systemic AP. First, actual operating pressure and SNAs under baroreflex closed-loop conditions in the 0° supine posture were obtained. The animal was kept in the 0° supine posture for 10 min while CSP was matched with systemic AP via the servo-controlled piston pump.

Second, the static characteristics of the sympathetic baroreflex system were estimated in the 0° position under baroreflex open-loop conditions. The animal was kept in the 0° supine posture while CSP was decreased to 40 mmHg and then increased stepwise from 40 to 160 mmHg in increments of 20 mmHg. Each CSP step was maintained for 60 s.

Third, actual operating pressure and SNAs under baroreflex closed-loop conditions in the 60° upright tilt position were obtained. The animal was kept supine for 10 min and then tilted upright to 60° within 10 s by inclining the tilt bed to 60° and dropping the lower regions of the rabbit with the fulcrum set at the level of the carotid sinus. The 60° upright posture was maintained for 10 min. CSP was matched with systemic AP via the servo-controlled piston pump. Since the clothes-like bag stabilized the posture of the animals, there was no additional mechanical movement that reduced the quality of measurements. The position of the head remained almost fixed during the tilt to minimize vestibular stimulation. Last, the static characteristics of the sympathetic baroreflex system were estimated during the 60° upright tilt posture. CSP was increased stepwise from 40 to 160 mmHg similarly to the experiment in the 0° position. These SNAs and AP were recorded at a 200-Hz sampling rate using a 12-bit analog-to-digital converter and stored on the hard disk of a dedicated laboratory computer system for later analysis.

Data analysis. The SNA signals were normalized by the following steps. First, for each type of SNA, 0 arbitrary unit (a.u.) was assigned to the postmortem noise level. Second, 100 a.u. were assigned to the average of actual operating SNA values during baseline period in 0° positions. Last, the other SNA signals were then normalized to these values in each experiment.

These SNA and HR values were averaged for the last 10 s of each CSP level. The static relationships between CSP and SNA and between CSP and HR were parameterized by two widely used traditional models (nonlinear reverse-sigmoidal curve, linear regression line), although both models have limited abilities to reproduce the actual data. In the former case, the data were parameterized by a four-parameter logistic equation model as follows:

$$Y = P_4 + \frac{P_1}{1 + \exp[P_2(CSP - P_3)]} \quad (1)$$

where Y is SNA or HR, P_1 is the response range of Y (i.e., the difference between the maximum and minimum values of Y), P_2 is the coefficient of gain, P_3 is the midpoint CSP of the logistic function, and P_4 is the minimum value of Y. We calculated the instantaneous gain

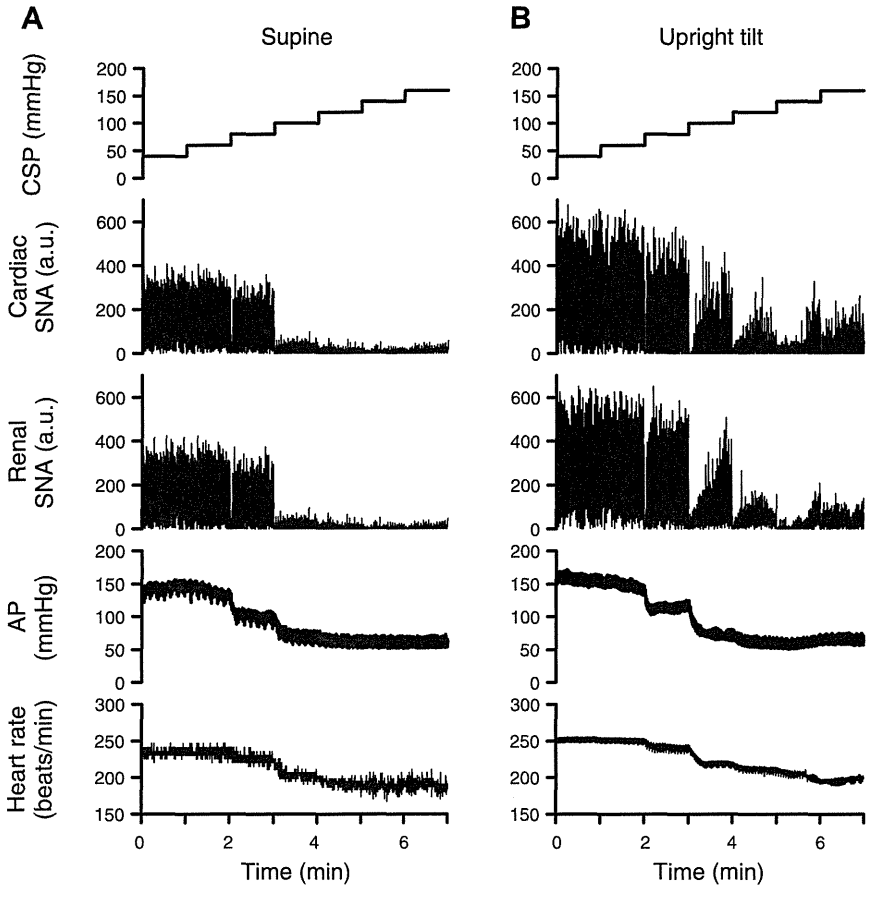

Fig. 1. Representative time series of renal and cardiac sympathetic nerve activities (SNAs) and arterial pressure (AP) in response to a stepwise increase in intracarotid sinus pressure (CSP) in 0° supine (*A*) and 60° upright tilt postures (*B*) obtained from 1 animal. Each CSP step was maintained for 1 min. All data were sampled at 10 Hz. In both SNAs, increasing CSP decreased SNAs in both postures, but upright tilt increased SNAs at all CSP levels. a.u., Arbitrary unit.

from the first derivative of the logistic function and the maximum gain (G_{max}) from $-P_1P_2/4$ at CSP = P_3.

Statistic analysis. All data are means ± SD. Effects of the upright tilt on baroreflex parameters were evaluated by repeated-measures analysis of variance. When the main effect was found to be significant, post hoc multiple comparisons were made using Scheffé's *F*-test to compare baroreflex controls between renal and cardiac SNAs (3). Differences were considered significant when $P < 0.05$.

RESULTS

Baroreflex control of renal and cardiac SNAs. Figure 1 shows the representative time series data obtained from one subject. The renal and cardiac SNAs similarly decreased in response to stepwise increase in CSP in the 0° supine posture (Fig. 1*A*). The 60° upright tilt increased these SNAs at each CSP level (Fig. 1*B*) compared with the supine posture.

Figure 2 shows the relationship between CSP and SNA in the same data as in Fig. 1*A*. In Fig. 2, these SNAs were averaged for the last 10 s of each CSP level to investigate the steady-state, not transient, response to a stepwise change in CSP. The 60° upright tilt increased renal (Fig. 2*A*) and cardiac SNAs (Fig. 2*C*) at all CSP levels compared with the supine posture. The renal SNA approximately matched the cardiac SNA at all CSP levels in the supine posture (Fig. 2*B*) and also in the upright tilt posture (Fig. 2*D*).

When the static relationship between CSP and each SNA was fitted to a nonlinear reverse-sigmoidal curve (Fig. 3), the r^2 value was ~0.95. The 60° upright tilt shifted the CSP-renal SNA curve upward to a higher SNA (Fig. 3*A*). Similarly, the upright tilt shifted the CSP-cardiac SNA curve (Fig. 3*C*) in the same manner as renal SNA. The CSP-renal SNA curve was almost superimposed on the CSP-cardiac SNA curve in the 0° supine (Fig. 3*B*) and upright tilt postures (Fig. 3*D*). However, the model was limited in reproducing the data, since the measured SNAs did not saturate at the CSP levels of 40–60 mmHg.

When the static relationship between CSP and each SNA was fitted to a linear regression line (Fig. 4), the r^2 value was 0.82–88, lower than when the nonlinear reverse-sigmoidal curve was used. The 60° upright tilt shifted the CSP-renal SNA (Fig. 4*A*) and the CSP-cardiac SNA lines (Fig. 4*C*) upward to the higher SNA levels. The CSP-renal SNA line was almost superimposed on the CSP-cardiac SNA line in the 0° supine (Fig. 4*B*) and upright tilt postures (Fig. 4*D*).

Averaged data from all animals showed that the 60° upright tilt increased renal (Fig. 5*A*) and cardiac SNAs (Fig. 5*B*) at all CSP levels compared with the 0° supine posture. The renal SNA almost matched the cardiac SNA at all CSP levels in the supine (Fig. 5*D*) and also in the upright tilt posture (Fig. 5*E*),

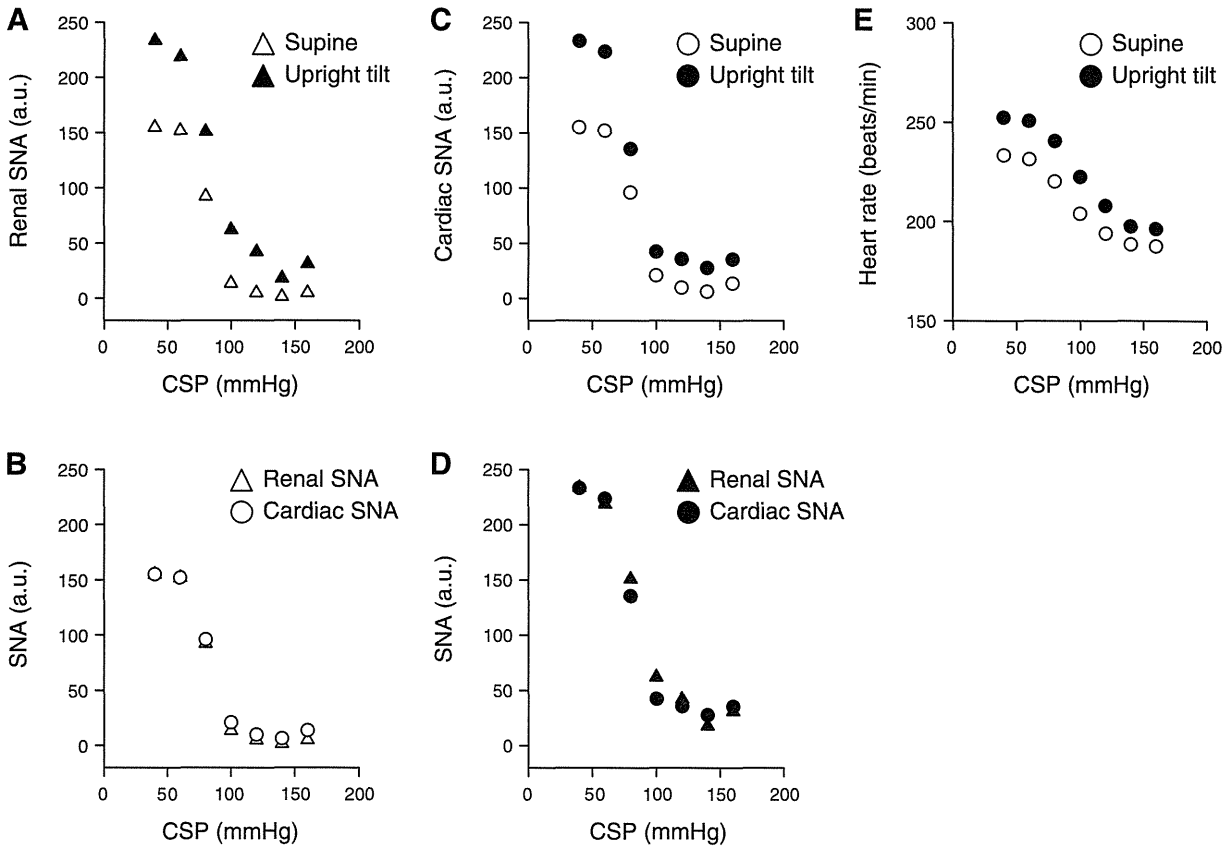

Fig. 2. Example of arterial baroreflex control of renal (*A*) and cardiac SNAs (*C*) and heart rate (HR; *E*). Data were obtained from the same animal studied in Fig. 1 and averaged for the last 10 s of each CSP level. Open and filled symbols show the data in the supine and 60° upright tilt postures, respectively. The upright tilt shifted the baroreflex control of SNA to a higher SNA similarly in the CSP-renal SNA (*A*) and CSP-cardiac SNA relationships (*C*). Data in *B* and *D* represent the superimposing of baroreflex control of SNA between renal and cardiac SNAs in both the supine and upright tilt postures, respectively. The upright tilt also shifted the baroreflex control of HR upward (*E*).

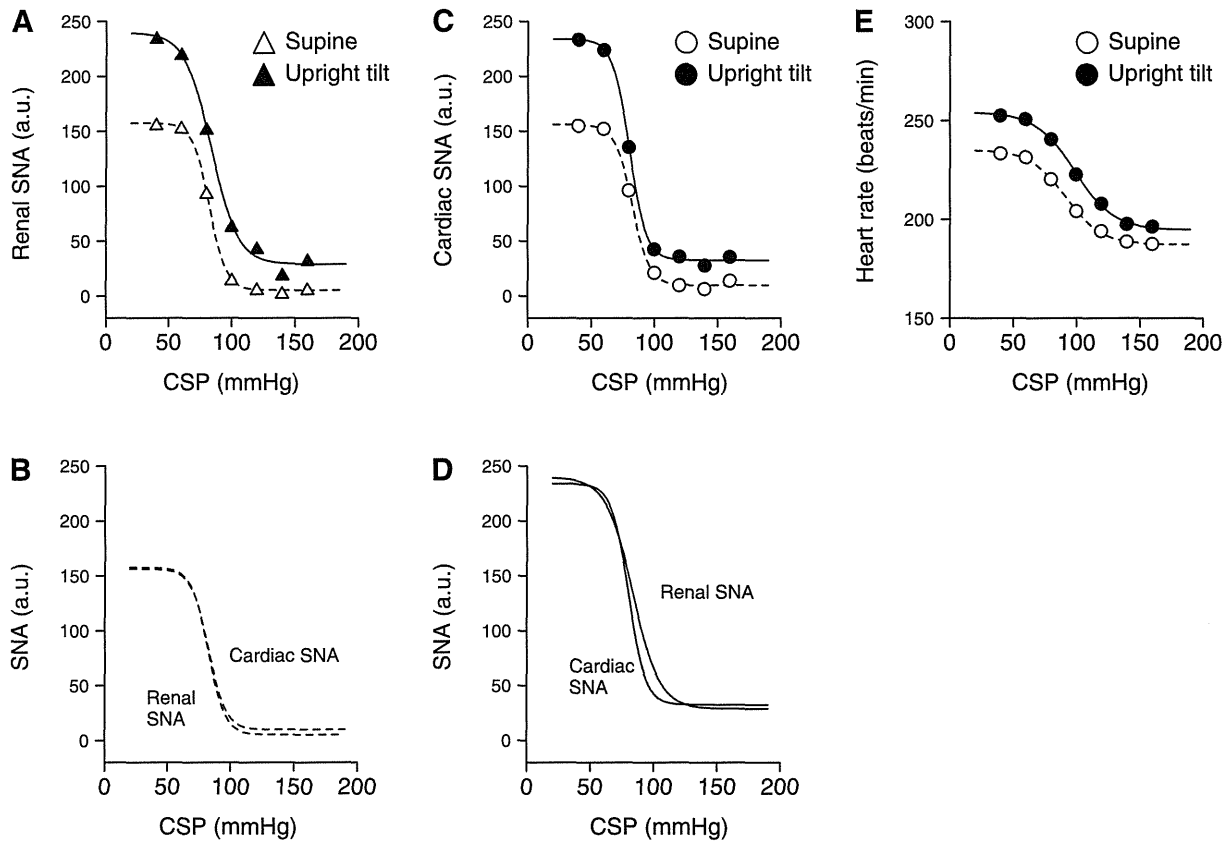

Fig. 3. Example of a model of the data shown in Fig. 2 using reverse-sigmoid 4-parameter logistic functions. Dotted and solid curves show the data in the supine and 60° upright tilt postures, respectively. The upright tilt shifted the baroreflex curves to a higher SNA similarly in renal (*A*) and cardiac SNAs (*C*). The curves were superimposed between these SNAs in the supine (*B*) and upright tilt postures (*D*). The upright tilt also shifted the baroreflex curve of HR upward (*E*).

indicating that 60° upright tilt shifted the CSP-SNA relationship upward by similar magnitudes in renal and cardiac SNAs.

When the static relationship between CSP and each SNA was fitted to a nonlinear reverse-sigmoidal curve (Fig. 6), the upright tilt shifted the CSP-SNA curve to higher SNA similarly in renal (Fig. 6*A*) and cardiac SNAs (Fig. 6*C*). The CSP-SNA relationship was almost superimposed between these SNAs in both the supine (Fig. 6*B*) and upright tilt postures (Fig. 4*D*). In both renal and cardiac SNAs, P_1 (the range of SNA response to CSP), P_4 (the minimum value of SNA), and the maximal gain (at the midpoint of the logistic function) were larger at upright tilt than supine posture (Table 1), whereas P_2 (the coefficient of gain) and P_3 (the midpoint CSP of the logistic function) were not different between postures (Table 1). In both postures, these parameters of P_{1-4} and maximal gain were similar in renal and cardiac SNAs (Table 1).

When the static relationship between CSP and each SNA was fitted to a linear regression line (Fig. 7), the upright tilt shifted the CSP-SNA line to higher SNA similarly in renal (Fig. 7*A*) and cardiac SNAs (Fig. 7*C*). It increased the slope of regression from -1.4 ± 0.3 to -1.8 ± 0.3 a.u./mmHg in renal SNA and from -1.4 ± 0.3 to -1.8 ± 0.4 a.u./mmHg in cardiac SNA. The CSP-SNA lines were almost superimposed on their SNAs in the 0° supine (Fig. 7*B*) and also the upright tilt posture (Fig. 7*D*). In both SNAs of all animals, the r^2 value was always lower (0.80–0.89) than when a nonlinear reverse-sigmoidal curve was used (0.92–0.97).

In addition, in both 0° supine and 60° upright tilt postures, scatter plotting of cardiac SNA over renal SNA was approximately close to the line of identity for each subject (Fig. 8A) and the pooled data from all subjects (Fig. 8*B*), indicating that these SNAs changed in parallel in response to stepwise increase in CSP regardless of posture. The upright tilt did not change operating AP (steady-state AP: 102 ± 4 mmHg in supine posture, 102 ± 5 mmHg in upright tilt posture). The upright tilt increased operating renal (100 a.u in supine posture, 148 ± 19 a.u. in upright posture) and cardiac SNAs (100 a.u in supine posture, 155 ± 21 a.u. in upright posture) by similar magnitudes.

Figure 9 showed the discharge characteristics of the renal and cardiac SNAs obtained from the same animal studied in Fig. 1. These SNAs were similar to some extent regardless of baroreflex condition and posture. In the supine posture (Fig. 9*A*), first, these SNAs were weakly pulse synchronous and had slower fluctuations with a time cycle of ~1.7 s in the baroreflex closed-loop condition, where CSP was artificially matched with systemic AP. The CSP and AP also had fluctuations with the same time cycle. Second, in the baroreflex open-loop condition, where CSP was fixed at 40 mmHg (the CSP level was chosen because it maximized these SNAs) without pulse, these SNAs had neither a pulse rhythmicity nor the slower fluctuation observed in the closed-loop condition. These discharge characteristics of SNAs were also observed in the 60° upright posture (Fig. 9*B*), although the amplitude of SNAs were larger at upright tilt than supine posture.

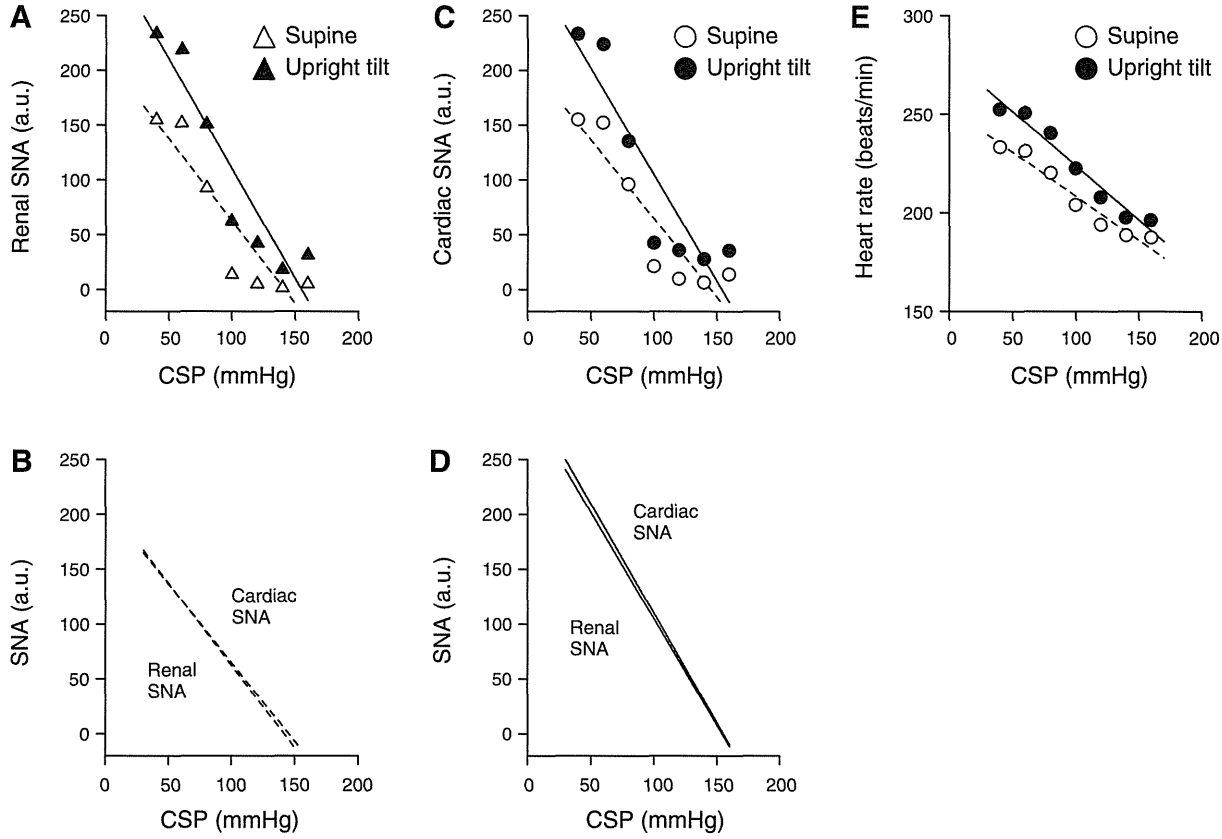

Fig. 4. Example of a model of the data shown in Fig. 2 using a simple regression line. Dotted and solid lines show the data in the supine and 60° upright tilt postures, respectively. The upright tilt shifted the baroreflex lines to a higher SNA similarly in renal (*A*) and cardiac SNAs (*C*). The lines were superimposed between these SNAs in the supine (*B*) and upright tilt postures (*D*). The upright tilt also shifted the baroreflex line of HR upward (*E*).

Baroreflex control of HR. In the representative time-series data, HR decreased in response to a stepwise increase in CSP in the 0° supine posture (Fig. 1*A*) and during 60° upright tilt (Fig. 1*B*). The upright tilt shifted the CSP-HR relationship upward to a higher HR (Fig. 2*E*), although HR was averaged for the last 10 s of each CSP level to investigate the steady-state, not transient, response to stepwise change in CSP.

Averaged data from all animals showed that the upright tilt shifted the CSP-HR relationship upward to a higher HR (Fig. 5*E*). When the static relationship between CSP and HR was fitted to a nonlinear reverse-sigmoidal curve (Fig. 6*E*), the P_1 (the range of HR response to CSP) and the maximal gain (at the midpoint of the logistic function) were larger at upright tilt than in the supine posture (Table 2), whereas P_2 (the coefficient of gain), P_3 (the midpoint CSP of the logistic function), and P_4 (the minimum value of HR) were not different between postures (Table 2). When the static relationship between CSP and HR was fitted to a linear regression line (Fig. 8*E*), the upright tilt increased the slope of regression from 0.46 ± 0.3 to 0.60 ± 0.3 beats·min^{-1}·mmHg^{-1}. The upright tilt increased operating HR (steady-state HR; 204 ± 11 beats/min in supine posture, 220 ± 12 beats/min in upright tilt posture).

DISCUSSION

Arterial baroreflex control of SNA is considered to have an important role to maintain AP under orthostatic stress against gravitational fluid shift directed toward the lower part of the body (15). In addition, we (8) recently reported that upright tilt resets arterial baroreflex control of renal SNA to increase orthostatic sympathetic activation. However, it remains unknown whether upright tilt resets arterial baroreflex control of SNA innervating to cardiovascular organs (i.e., the heart) other than the kidney. One major new finding in this study is that 60° upright tilt resets arterial baroreflex control of SNA to higher SNA similarly in renal and cardiac SNAs. This supports our hypothesis that upright tilt causes a parallel resetting of arterial baroreflex control of renal and cardiac SNAs in anesthetized rabbits.

Some regional differences between renal and cardiac SNAs certainly have been reported under some physiological conditions. First, for example, the dynamic high-pass characteristics in baroreflex control of SNA were greater in cardiac SNA than renal SNA (6, 10). Second, activating left atrial receptors increased cardiac SNA but decreased renal SNA (9). Last, hypoxia reset the AP-SNA relationship to higher AP and SNA in renal SNA but to lower AP and SNA in cardiac SNA (4). These lines of evidence indicate that renal and cardiac SNAs respond differently to specific physiological stimulation and stress (14).

However, our results indicate that upright posture induces a parallel resetting in arterial baroreflex control of renal and cardiac SNAs in the static characteristics. In agreement with previous studies (6, 7), the CSP-renal SNA reverse-sigmoidal curve was superimposable to the CSP-cardiac SNA curve in

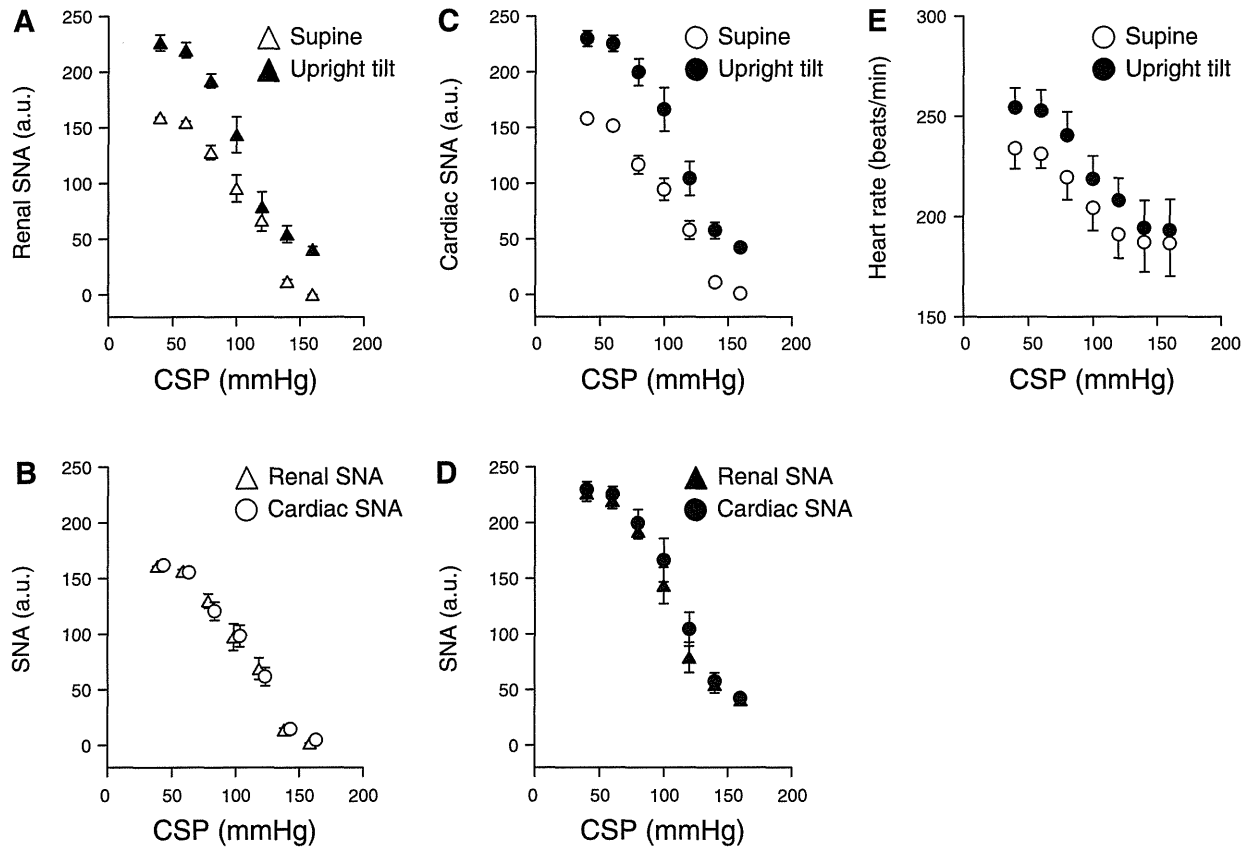

Fig. 5. Averaged data of arterial baroreflex control of renal (*A*) and cardiac SNAs (*C*) and HR (*E*) from all animals (n = 8). Open and filled symbols show the data in the supine and 60° upright tilt postures, respectively. The upright tilt shifted the baroreflex control of SNA to a higher SNA similarly in the CSP-renal SNA (*A*) and CSP-cardiac SNA relationships (*C*). *B* and *D* represent the superimposing of baroreflex control of SNA between renal and cardiac SNAs in both the supine and upright tilt postures, respectively. The upright tilt also shifted the baroreflex control of HR upward (*E*). Data are means ± SD.

the supine posture. This indicates that static nonlinear characteristics in arterial baroreflex control of renal SNA matched those of cardiac SNA in the posture. In addition, since upright tilt posture shifted the CSP-SNA curves upward similarly in renal and cardiac SNAs, the static nonlinear characteristics in arterial baroreflex control of renal SNA also matched those of cardiac SNA in upright tilt posture. These results were consistent with the close correlation between renal and cardiac SNAs during forced CSP changes with supine and upright tilt postures. They might also be consistent with a numerical simulation study indicating parallel responses of renal and cardiac SNAs to physiological pressure perturbations (AP change) (6).

Our results indicate that upright posture resets arterial baroreflex control of HR to a higher HR. This is consistent with the results of baroreflex resetting for cardiac SNA under upright tilt, because the P_1 (the response range) and the maximal gain (at the midpoint of the logistic function) were larger in both CSP-HR and CSP-cardiac SNA relationships. The parallelism suggests that cardiac sympathetic efferent was a dominant determinant for HR in the present experimental condition with cutting of vagal nerves. Our results could be consistent with the increase in the baroreflex gain for HR assessed by a neck pressure/suction device in humans (11).

Limitations. The present study has several limitations. First, we excluded the efferent effect of vagally mediated arterial baroreflex and an anesthetic agent that could affect baroreflex control of SNA. Second, the vascular isolation of carotid sinus might decrease brain blood flow under, in particular, upright tilt position. Third, we eliminated cardiopulmonary baroreflex by cutting bilateral vagal nerves. Earlier human studies have indicated that nonhypotensive hypovolemic perturbations do not change AP but reduce central venous, right heart, and pulmonary pressures and cause vasoconstriction. These observations have been interpreted as reflexes triggered by cardiopulmonary baroreceptors (5, 12). However, Taylor et al. (17) showed that small reductions of effective blood volume reduce aortic baroreceptive areas and trigger hemodynamic adjustments that are so efficient that alterations in AP escape detection by conventional means. In addition, Fu et al. (2) reported that arterial baroreceptors are consistently unloaded during low levels (i.e., −10 and −15 mmHg) of lower body negative pressure in humans. Accordingly, further studies are needed to understand the relative importance and mutual cooperation of arterial and cardiopulmonary baroreflexes in AP control during orthostatic stress. Fourth, we investigated arterial baroreflex during upright posture in rabbits, which are quadripeds. However, denervation of both carotid and aortic arterial baroreflexes caused postural hypotension of ~50 mmHg during 60° upright tilt in quadripeds [rabbits and rats (16)]. This suggests that even in quadripeds, arterial baroreflex has a very important role in maintenance of AP under orthostatic stress.

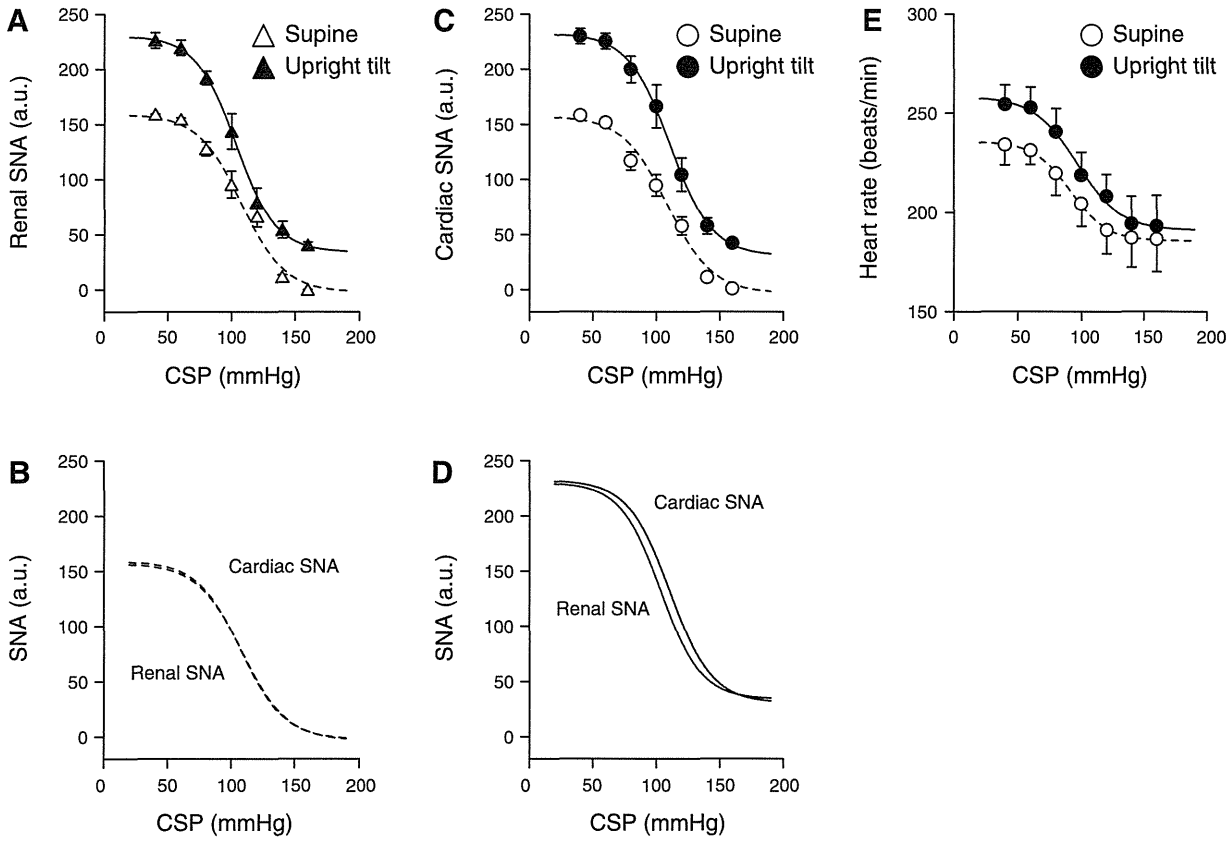

Fig. 6. A model of the averaged data shown in Fig. 5 using reverse-sigmoid 4-parameter logistic functions. Dotted and solid curves show the data in the supine and 60° upright tilt postures, respectively. The upright tilt shifted the baroreflex curves to a higher SNA similarly in renal (*A*) and cardiac SNAs (*C*). The curves were superimposed between these SNAs in the supine (*B*) and upright tilt postures (*D*). The upright tilt also shifted the baroreflex curve of HR upward (*E*).

Last, although we used two widely used traditional models to analyze the relationship between CSP and SNA, both have limited abilities to reproduce actual data. The nonlinear reverse-sigmoidal curve parameterized by a four-parameter logistic equation model provided high r^2 values (0.92–0.97) regardless of SNA type and posture. However, we failed to observe a saturation of SNA at the lowest CSP level in some cases (40 mmHg; Fig. 3, *A* and *B*, in upright tilt position). Lots of earlier studies have applied the model to AP and SNA (or HR) data under pharmacological perturbation (i.e., nitroprusside, phenylephrine) (1, 14), although it is difficult to observe clear saturation and/or threshold in the data. In contrary, the simple linear regression line model provided lower r^2 values (0.80–0.89). The plotted data did not appear to lie on a simple line in individuals (Fig. 4). Accordingly, we cannot conclude whether the relation between CSP and SNA is sigmoid or not. This problem is not the purpose of this study. Importantly, without modeling, our data (Fig. 2 and 5) indicate the parallel resetting of arterial baroreflex control of renal and cardiac SNAs.

Table 1. *Effect of upright tilt on parameters of baroreflex control of renal and catdiac SNAs*

	Supine	Upright tilt
Renal SNA		
P_1, a.u.	161 ± 2	196 ± 5*
P_2, a.u./mmHg	0.08 ± 0.01	0.08 ± 0.02
P_3, mmHg	105 ± 6	104 ± 6
P_4, a.u.	2 ± 1	34 ± 6*
G_{max}, a.u./mmHg	−1.5 ± 0.4	−1.9 ± 0.4*
Cardiac SNA		
P_1, a.u.	160 ± 2	201 ± 5*
P_2, a.u./mmHg	0.08 ± 0.01	0.08 ± 0.02
P_3, mmHg	109 ± 6	111 ± 6
P_4, a.u.	2 ± 1	31 ± 6*
G_{max}, a.u./mmHg	−1.4 ± 0.4	−1.9 ± 0.4*

Values are means ± SD (n = 8) for the parameters of baroreflex control of renal and cardiac sympathetic nerve activities (SNAs). See *Eq. 1* in METHODS for definitions of the 4 parameters of the logistic function. *$P < 0.05$, supine vs. upright tilt.

In conclusion, upright posture causes a resetting in arterial baroreflex control of SNA in parallel in renal and cardiac SNAs in anesthetized rabbits.

GRANTS

This study was supported by a research project promoted by the Ministry of Health, Labour and Welfare in Japan (no. H18-nano-ippan-003, H21-nano-ippan-005), a Grant-in-Aid for Scientific Research promoted by the Ministry of Education, Culture, Sports, Science and Technology in Japan (no. 20390462), and the Industrial Technology Research Grant Program from the New Energy and Industrial Technology Development Organization (NEDO) of Japan.

DISCLOSURES

No conflicts of interest, financial or otherwise, are declared by the author(s).